Chapter

12 Image Processing

Image processing is a computational process that transforms one or more input images into an output image. Image processing is frequently used to enhance an image for *human* viewing or interpretation, for example to improve contrast. Alternatively, and of more interest to robotics, it is the foundation for the process of feature extraction which will be discussed in much more detail in the next chapter.

An image is a rectangular array of picture elements (pixels) so we will use a MATLAB® matrix to represent an image in the workspace. This allows us to use MATLAB's powerful and efficient armoury of matrix operators and functions.

We start in Sect. 12.1 by describing how to load images into MATLAB® from sources such as files (images and movies), cameras and the internet. We then discuss various classes of image processing algorithms. These algorithms operate pixel-wise on a single image or a pair of images, or on local groups of pixels within an image and we refer to these as monadic, diadic, and spatial operations respectively. Monadic and diadic operations are covered in Sect. 12.2 and 12.3. Spatial operators are described in Sect. 12.4 and include operations such as smoothing, edge detection, and template matching. A closely related technique is shape-specific filtering or mathematical morphology and this is described in Sect. 12.5. Finally in Sect. 12.6 we discuss shape changing operations such as cropping, shrinking, expanding, as well as more complex operations such as rotation and generalized image warping.

Robots will always gather imperfect images of the world due to noise, shadows, reflections and uneven illumination. In this chapter we discuss some fundamental tools and "tricks of the trade" that can be applied to real-world images.

12.1 Obtaining an Image

Today digital images are ubiquitous. We obtain them quickly and easily using our digital cameras, our phones and our laptops, and have personal collections of thousands or tens of thousands of images. Beyond our personal collections are massive online collection of digital images such as Google Images, Picasa or Flickr which also have metadata describing the image content and increasingly its geographic location. Images of Earth from space, the Moon and Mars are also available. We also have access to live image streams from other people's cameras – there are tens of thousands of webcams around the world capturing images and broadcasting them on the internet.

12.1.1 Images from Files

We start with images stored in files since it is very likely that you already have lots of images stored on your computer. In this chapter we will work with some images provided with the Toolbox, but you can easily substitute your own images. We import an image into the MATLAB® workspace using the Toolbox function `iread`

```
>> street = iread('street.png');
```

which returns a matrix

```
>> about(street)
street [uint8] : 851x1280 (1089280 bytes)
```

which has 851 rows and 1 280 columns. We normally describe the dimensions of an image in terms of its width × height, so this would be a 1 280 × 851 pixel image.

> In Chap. 11 we wrote the coordinates of a pixel as (u, v) which are the horizontal and vertical coordinates respectively. In MATLAB® this is the matrix element (v, u) – note the reversal of coordinates. Note also that the top-left pixel is (1, 1) in MATLAB® not (0, 0).

This image was read from a file called `street.png` which is in portable network graphics (PNG) format – a lossless compression format▸ widely used on the internet. The function `iread` searches for the image in the current folder, and then in each folder along your MATLAB® path.▸ This particular image has no color, it is a greyscale or monochromatic image.

Lossless means that the compressed image, when uncompressed, will be exactly the same as the original image.

The example images are kept within the `images` folder of the Machine Vision Toolbox distribution which is automatically searched by the `iread` function.

The `about` command used above indicates that the matrix `street` belongs to the class `uint8` – the elements of the matrix are unsigned 8-bit integers in the interval [0, 255]. The elements are referred to as pixel values or grey values and are proportional to the luminance of that point in the original scene. For this 8-bit image the pixel values vary from 0 (darkest) to 255 (brightest). For example the pixel at image coordinate (300,200) is

```
>> street(200,300)
ans =
   42
```

which is quite dark – the pixel corresponds to a point in the closest doorway.

For some image processing operations that we will consider later it is useful to consider the pixel values as floating point numbers. In this case each pixel is an 8-byte MATLAB® double precision number in the range [0, 1]. We can convert a `uint8` class image to a floating point image by

```
>> street_d = idouble(street);
>> about(street_d)
street_d [double] : 851x1280 (8714240 bytes)
```

Alternatively we can specify this as an option when we load the image

```
>> street_d = iread('street.png', 'double');
```

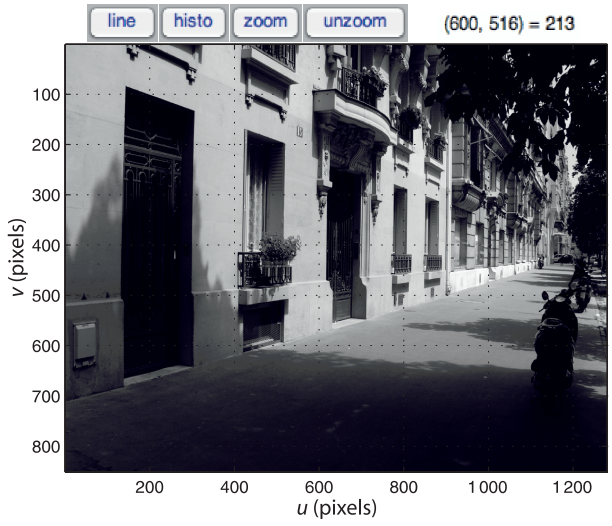

Fig. 12.1.
The `idisp` image browsing window. The top right shows the coordinate and value of the last pixel clicked on the image. The buttons at the top left allow the pixel values along a line to be plotted, a histogram to be displayed, or the image to be zoomed

The **dynamic range** of a sensor is the ratio of its largest value to its smallest value. For images it is useful to express the $\log_2$ of this ratio which makes it equivalent to the photographic concepts of stops or exposure value. Each photosite contains a charge well in which photon-generated electrons are captured during the exposure period (see page 260). The charge well has a finite capacity before the photosite saturates and this defines the maximum value. The minimum number of electrons is not zero but a finite number of thermally generated electrons.

An 8-bit image has a dynamic range of around 8 stops, a high-end 10-bit camera has a range of 10 stops, and negative film is perhaps in the range 10–12 stops but is quite non-linear.

At a particular state of adaptation, the human eye has a range of 10 stops, but the total adaptation range is an impressive 20 stops. This is achieved by using the iris and slower (tens of minutes) chemical adaptation of the sensitivity of rod cells. Dark adaptation to low luminance is slow, from bright Sun to a dark room takes many minutes. Adaptation from dark to bright is faster but sometimes painful.

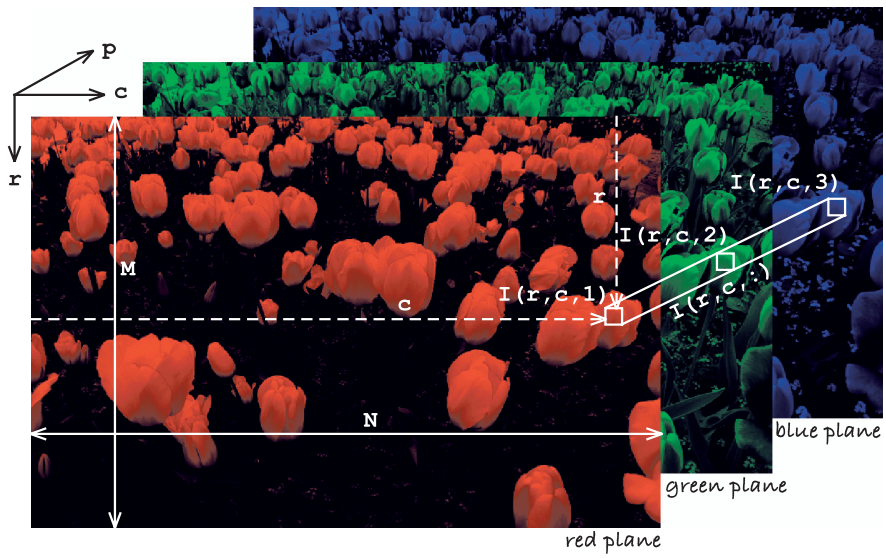

Fig. 12.2. Color image shown as a 3-dimensional structure with dimensions: row, column, and color plane

A tool that we will see and use a lot to display an image is `idisp`

```
>> idisp(street)
```

which displays the matrix as an image and allows interactive inspection of pixel values as shown in Fig. 12.1. Clicking on a pixel will display the pixel coordinate and its grey value in the top right of the window. The image can be zoomed (and unzoomed) and we can display a histogram or the intensity profile along a line between any two selected points. It has many options and these are described in the online documentation.

We can just as easily load a color image

```
>> flowers = iread('flowers8.png');
>> about(flowers)
flowers [uint8] : 426x640x3 (817920 bytes)
```

which is a 3-dimensional matrix of `uint8` values as shown in Fig. 12.2. The color of each pixel is represented as an RGB tristimulus which is a 3-vector. For example the pixel at (318, 276)

```
>> pix = flowers(276,318,:)
ans(:,:,1) =
    57
ans(:,:,2) =
    91
ans(:,:,3) =
   198
```

has a tristimulus value (57, 91, 198). This pixel corresponds to one of the small blue flowers and has a large blue component. We can display the image and examine it interactively using `idisp` and clicking on a pixel will display its tristimulus value.

The variable `pix` has been displayed by MATLAB® in an unusual and non-compact manner. This is because the pixel value is

```
>> about(pix)
pix [uint8] : 1x1x3 (3 bytes)
```

a $1 \times 1 \times 3$ matrix. The first two dimensions are called singleton dimensions and we can *squeeze* them out

```
>> squeeze(pix)'
ans =
   57   91  198
```

which results in a more familiar 3-vector.

The third dimension of the image shown in Fig. 12.2 is known as the color plane index. For example

```
>> idisp( flowers(:,:,1) )
```

would display the red color plane as a greyscale image that shows the red stimulus at each pixel. The index 2 or 3 would select the green or blue plane respectively.

The tristimulus values are of type `uint8` in the range [0, 255] but the image can be converted to double precision values in the range [0, 1] using the `'double'` option to `iread` or by applying the function `idouble` to the integer color image, just as for a greyscale image. The option `'grey'` ensures that a greyscale image is returned irrespective of whether or not the file contains a color image.▸

Using ITU Rec. 709 by default. See also the function `imono`.

The `iread` function can also accept a wildcard filename allowing it to load a sequence of files. For example

```
>> seq = iread('seq/*.png');
>> about(seq)
seq [uint8] : 512x512x9 (2359296 bytes)
```

loads nine images in PNG format from the folder `seq`. The result is a 3-dimensional matrix and the last index represents the image number within the sequence. That is `seq(:,:,k)` is the k^{th} image in the sequence and is a 512×512 greyscale image. In terms of Fig. 12.2 the images in the sequence extend in the `p` direction. If the images were color then the result would be a 4-dimensional matrix where the last index represents the image number within the sequence, and the third index represents the color plane.

If `iread` is called with no arguments a file browsing window pops up allowing navigation through the file system to find the image. The function also accepts a URL allowing it to load an image, but not a sequence, from the web. The function can read most common image file formats including JPEG, TIFF, GIF, PNG, PGM, PPM, PNM. Other options for `iread` are described in the online documentation.

A very large number of **image file formats** have been developed and are comprehensively catalogued at http://en.wikipedia.org/wiki/Image_file_formats. The most popular is JPEG which is used for digital cameras and webcams. TIFF is common in many computer systems and often used for scanners. PNG and GIF are widely used on the web. The internal format of these files are complex but a large amount of good quality open-source software exists in a variety of languages to read and write such files. MATLAB® is able to read many of these image file formats.

A much simpler set of formats, widely used on Unix systems, are PBM, PGM and PPM (generically PNM) which represent images without compression, and optionally as readable ASCII text. A host of open-source tools such as ImageMagick provide format conversions and image manipulation under Unix, MacOS X and Windows.

12.1.2 Images from an Attached Camera

Most laptop computers today have a builtin camera for video conferencing. For computers without a builtin camera an external camera can be easily attached via a USB or FireWire connection. The means of accessing a camera is operating system specific and the Toolbox provides a simple interface to a camera for MacOS, Linux and Windows. A list of all attached cameras and their capability can be obtained by

```
>> VideoCamera('?')
```

We open a particular camera

```
>> cam = VideoCamera('name')
```

which returns an instance of a `VideoCamera` object that is a subclass of the `ImageSource` class. If name is not provided the first camera found is used. The constructor accepts a number of additional arguments such as `'grey'` which ensures that the returned image is greyscale irrespective of the camera type, and `'framerate'` which sets the number of frames captured per second.

The dimensions of the image returned by the camera are given by the `size` method

```
>> cam.size()
```

and an image is obtained using the `grab` method

```
>> im = cam.grab();
```

which waits until the next frame becomes available.◀

Since the frames are generated at a rate of R per second as specified by the `'framerate'` option, then the worst case wait is uniformly distributed in the interval $[0, 1/R)$.

12.1.3 Images from a Movie File

In Sect. 12.1.1 we loaded an image sequence into memory where each image came from a separate image file. More commonly image sequences are stored in a movie file format such as MPEG4 or AVI and it may not be practical or possible to keep the whole sequence in memory.

The Toolbox supports reading frames from a movie file stored in any of the popular formats such as AVI, MPEG and MPEG4. For example we can open a movie file

```
>> cam = Movie('traffic_sequence.mpg');
720 x 576 @ 2.999970e+01 fps
350 frames
```

JPEG employs *lossy* compression to reduce the size of the file. This means that the decompressed image isn't quite the same as the original image. It exploits limitations of the human eye and discards information that won't be noticed such as very small color changes (which are perceived less accurately than small changes in brightness) and fine texture. It is very important to remember that JPEG is intended for compressing images that will be *viewed by humans*. The loss of color detail and fine texture may be problematic for computer algorithms that analyze images.

JPEG was designed to work well for natural scenes but it does not do so well on lettering and line drawings with high spatial-frequency content. The degree of lossiness can be varied by adjusting the so-called quality factor which allows a tradeoff between image quality and file size. JPEG can be used for greyscale or color images.

What is commonly referred to as a JPEG file, often with an extension of `.jpg` or `.jpeg`, is more correctly a JPEG JFIF file. JFIF is the format of the file that holds a JPEG-compressed image as well as metadata. EXIF file format (Exchangeable Image File Format) is a standard for camera related metadata such as camera settings, time, location and so on. This metadata can be retrieved as a second output argument to `iread` as a cell array, or by using a command-line utility such as `exiftool` (http://www.sno.phy.queensu.ca/~phil/exiftool). See the Independent JPEG group web site http://www.ijg.org for more details.

which returns a `Movie` object that is an instance of a subclass of the `ImageSource` class and therefore polymorphic with the `VideoCamera` class just described. This movie has 350 frames and was captured at 30 frames per second.

The size of each frame within the movie is

```
>> cam.size()
ans =
   720   576
```

and the next frame is read from the movie file by

```
>> im = cam.grab();
>> about(im)
im [uint8] : 576x720x3 (1244160 bytes)
```

which is a 720 × 576 color image. With these few primitives we can write a very simple movie player

```
1      while 1
2          im = cam.grab;
3          if isempty(im), break; end
4          image(im)
5      end
```

where the test at line 3 is to detect the end of file, in which case `grab` returns an empty matrix.

The methods `nframes` and `framerate` provide the total number of frames and the number of frames per second. The methods `skiptotime` and `skiptoframe` provide an ability to move to desired frames within the movie.

12.1.4 Images from the Web

The term web camera has come to mean *any* USB or Firewire connected local camera but here we use it to refer to an *internet* connected camera that runs a web server that can deliver images on request. There are tens of thousands of these web cameras around the world that are pointed at scenes from the mundane to the spectacular. Given the URL of a webcam from Axis Communications▸ we can acquire an image from a camera anywhere in the world and place it in a matrix in our MATLAB® workspace.

Webcams support a variety of options that can be embedded in the URL and there is no standard for these. This function works only with recent webcams from Axis Communications.

For example we can connect to a camera at Dartmouth College in New Hampshire

```
>> cam = AxisWebCamera('http://wc2.dartmouth.edu');
```

which returns an `AxisWebCamera` object which is an instance of a subclass of the `ImageSource` class and therefore polymorphic with the `VideoCamera` and `Movie` classes previously described.

The image size in this case is

```
>> cam.size()
ans =
   480   640
```

Aspect ratio is the ratio of an image's width to its height. It varies widely across different imaging and display technologies. For 35 mm film it is 3:2 (1.5) which matches a 4 × 6" (1.5) print. Other print sizes have different aspect ratios: 5 × 7" (1.4), and 8 × 10" (1.25) which require cropping the vertical edges of the image in order to fit.

TV and early computer monitors used 4:3 (1.33), for example the ubiquitous 640 × 480 format. HDTV has settled on 16:9 (1.78). Modern digital SLR cameras typically use 1.81 which is close to the ratio for HDTV. In movie theatres very-wide images are preferred with aspect ratios of 1.85 or even 2.39. CinemaScope was developed by 20th Century Fox from the work of Henri Chrétien in the 1920s. An anamorphic lens on the camera compresses a wide image into a standard aspect ratio in the camera, and the process is reversed at the projector.

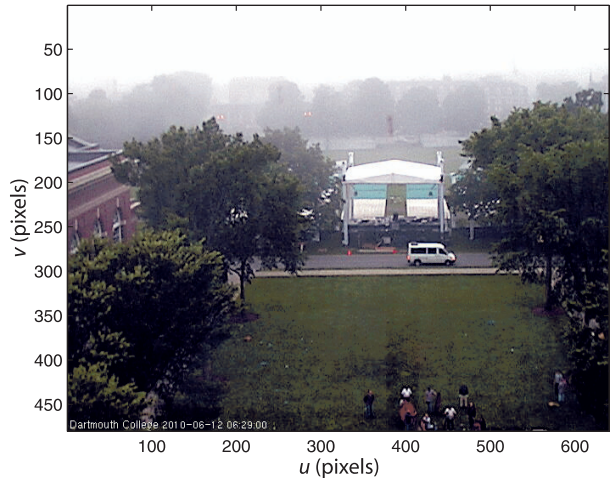

Fig. 12.3. An image from the Dartmouth University webcam which looks out over the main college green

and the next image is obtained by

```
>> im = cam.grab();
```

which returns a color image such as the one shown in Fig. 12.3. Webcams are configured by their owner to take pictures periodically, anything from once per second to once per minute. Repeated access will return the same image until the camera takes its next picture.

12.1.5 Images from Code

When debugging an algorithm it can be very helpful to start with a perfect and simple image before moving on to more challenging real-world images. The Toolbox function `testpattern` generates simple images with a variety of patterns including lines, grids of dots or squares, intensity ramps and intensity sinusoids. For example

```
>> im = testpattern('rampx', 256, 2);
>> im = testpattern('siny', 256, 2);
>> im = testpattern('squares', 256, 50, 25);
>> im = testpattern('dots', 256, 256, 100);
```

are shown in Fig. 12.4a. The second argument is the size of the of the created image, in this case they are all 256×256 pixels, and the remaining arguments are specific to the type of pattern requested. See the online documentation for details.

We can also construct an image from simple graphical primitives. First we create a blank *canvas* containing all black pixels (pixel value of zero)

```
>> canvas = zeros(200, 200);
```

Video file formats. Just as for image files there are a large number of different file formats for videos. The most common formats are MPEG and AVI. It is important to distinguish between the format of the file (the *container*), technically AVI is a file format, and the type of compression (the *codec*) used on the images within the file.

MPEG and AVI format files can be converted to a sequence of frames as individual files using tools such as FFmpeg and `convert` from the ImageMagick suite. The individual frames can then be loaded individually into MATLAB® for processing using `iread`. The Toolbox `Movie` class provides a more convenient way to read frames from common movie formats without having to first convert the movies to a set of individual frames.

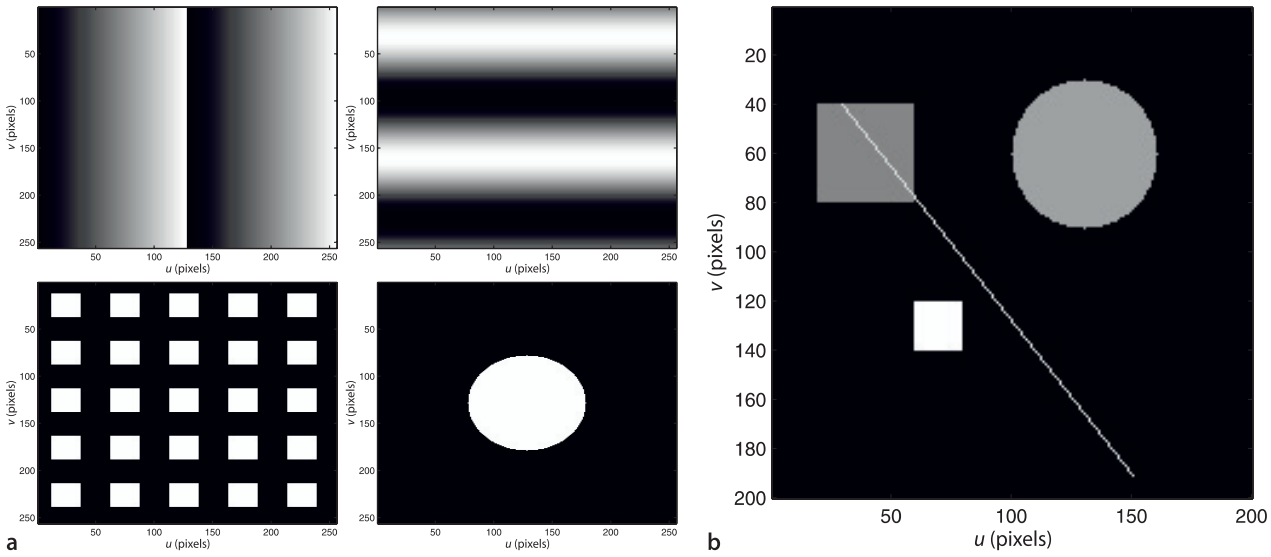

Fig. 12.4. Images from code. **a** Some Toolbox generated test patterns; **b** Simple image created from graphical primitives

and then we create two squares

```
>> sq1 = 0.5 * ones(40, 40);
>> sq2 = 0.9 * ones(20, 20);
```

The first has pixel values of 0.5 (medium grey) and is 40×40. The second is smaller (just 20×20) but brighter with pixel values of 0.9. Now we can paste these onto the canvas

```
>> canvas = ipaste(canvas, sq1, [20, 40]);
>> canvas = ipaste(canvas, sq2, [60, 120]);
```

where the last argument specifies the canvas coordinate (u, v) where the pattern will be pasted – the top-left corner of the pattern on the canvas. We can also create a circle

```
>> circle = 0.6 * kcircle(30);
```

of radius 30 pixels with a grey value of 0.6. The Toolbox function `kcircle` returns a square matrix

```
>> size(circle)
ans =
    61    61
```

of zeros with a centred maximal disk of values set to one. We can also paste that on to the canvas

```
>> canvas = ipaste(canvas, circle, [100, 30]);
```

Finally, we draw a line segment onto our canvas

```
>> canvas = iline( canvas, [30, 40], [150, 190], 0.8);
```

which extends from (30, 40) to (150, 190) and its pixels are all set to 0.8. The result

```
>> idisp(canvas)
```

is shown in Fig. 12.4b. We can clearly see that the shapes have different brightness, and we note that the line and the circle show the effects of quantization which results in a *steppy* or jagged shape.

> Note that all these functions take coordinates expressed in (u, v) notation not MATLAB® row column notation. The top-left pixel is (1, 1) not (0, 0).

12.2 Monadic Operations

Monadic image-processing operations are shown schematically in Fig. 12.5. The result is an image of the same size $W \times H$ as the input image, and each output pixel is a function of the corresponding input pixel

$$\boldsymbol{O}[u,v] = f\big(\boldsymbol{I}[u,v]\big), \quad \forall (u,v) \in \boldsymbol{I}$$

Since an image is represented by a matrix any MATLAB® element-wise matrix function or operator can be applied, for example scalar multiplication or addition, or functions such `abs` or `sqrt`.

The datatype of each pixel can be changed, for example from `uint8` (integer pixels in the range [0, 255]) to double precision values in the range [0, 1]

```
>> imd = idouble(im);
```

and vice versa

```
>> im = iint(imd);
```

A color image has 3-dimensions which we can also consider as a 2-dimensional image where each pixel value is a 3-vector. A monadic operation can convert a color image to a greyscale image where each output pixel value is a scalar representing the luminance of the corresponding input pixel

```
>> grey = imono(flowers);
```

The inverse operation is

```
>> color = icolor(grey);
```

which returns a 3-dimensional color image where each color plane is equal to `grey` – when displayed it is still appears as a monochrome image. We can create a color image where the red plane is equal to the input image by

```
>> color = icolor(grey, [1 0 0]);
```

which is a red tinted version of the original image.

Many monadic operations are concerned with altering the distribution of grey levels within the image. The distribution can be determined by computing the histogram of the image◂ which indicates the number of times each pixel value occurs. For example the histogram of the street scene is computed and displayed by

Which is not a monadic operator since the result is not an image. Technically it is form of feature extraction which is discussed in the next chapter.

```
>> ihist( street )
```

and the result is shown in Fig. 12.6a. We see that the grey values (horizontal axis) span the complete range from 0 to 255 but the distribution is far from uniform. By inspec-

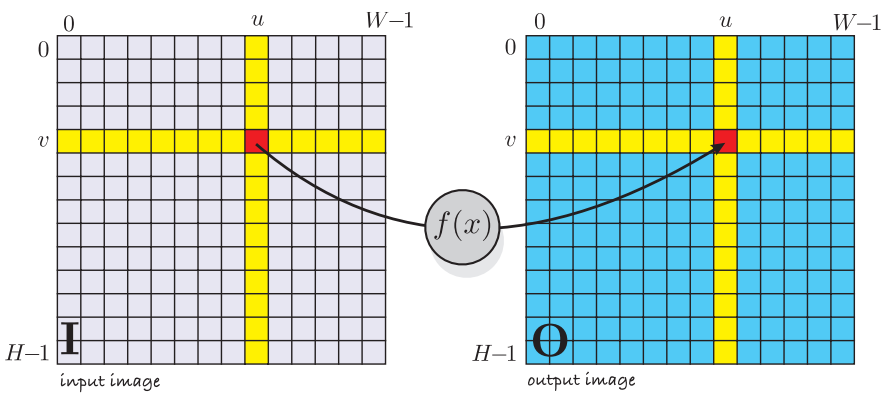

Fig. 12.5. Monadic image processing operations. Each output pixel is a function of the corresponding input pixel (shown in red)

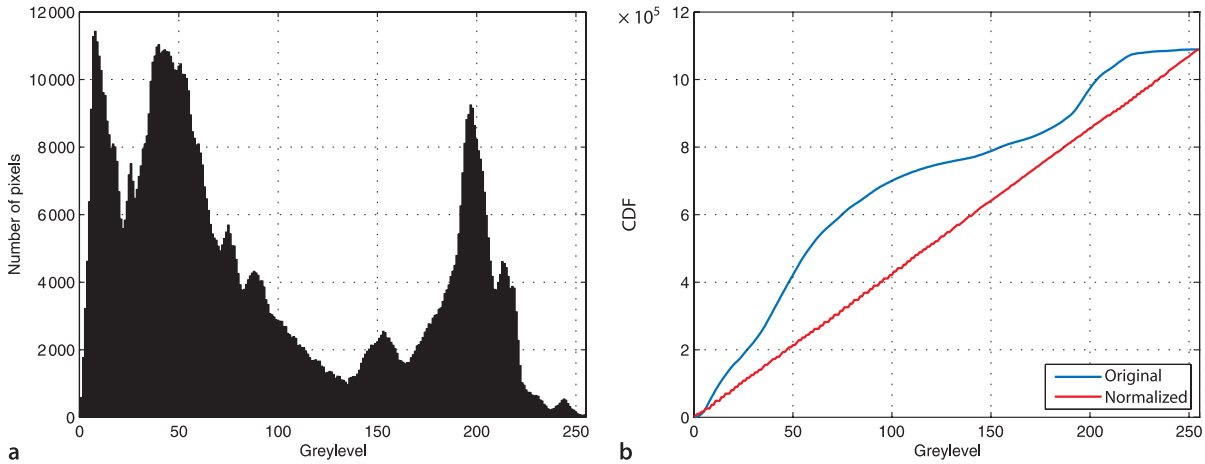

Fig. 12.6. Street scene. **a** Histogram, **b** cumulative histogram before and after normalization

tion we see that there are three significant peaks, but if we look more closely there are perhaps nine peaks, and if we zoomed right in we would see lots of very minor peaks. The concept of a peak depends on the scale at which we consider the data. We can obtain the histogram as a pair of vectors

```
>> [n,v] = ihist(street);
```

where the elements of `n` are the number of times pixels occur with the value of the corresponding element of `v`. The Toolbox function `peak` will automatically find the peaks

```
>> peak(n, v)'
ans =
     8    40    43    51   197    17    60    26    75   213
    88    92   218   176   153   108   111   147   113   119
   121   126   130   138   230   244
```

and in this case has found 26 peaks most of which are quite minor. Peaks that are *significant* are not only greater than their immediate neighbours they are greater than all other values *nearby* – the problem now is to specify what we mean by nearby. For example the peaks that are greater than all other values within ± 25 pixel values in the horizontal direction are

```
>> peak(n, v, 'scale', 25)'
ans =
     8    40   197
```

which are the three significant peaks that we observe by eye. The critical part of finding the peaks is choosing the appropriate scale. Peak finding is a topic that we will encounter again later and is also discussed in Appendix K.

The peaks in the histogram correspond to particular *populations* of pixels in the image. The peak around the greylevel of 40 for example corresponds to a large population of dark pixels which are mostly due to shadows. We can identify the pixels in this peak by a logical monadic operation

```
>> shadows = (street >= 30) & (street<= 80);
>> idisp(shadows)
```

and the resulting image is shown in Fig. 12.7b. All pixels that lie in the interval [30, 80] are shown as white. This image is of type `logical` but MATLAB® automatically converts logical true and false values to one and zero respectively when used in arithmetic operations. This is a rather simple, and adhoc, example of thresholding where we have selected certain pixels based just on their brightness.

Sometimes an image does not span the full range of available grey levels, for example an underexposed image will have no pixels with high values while an over-

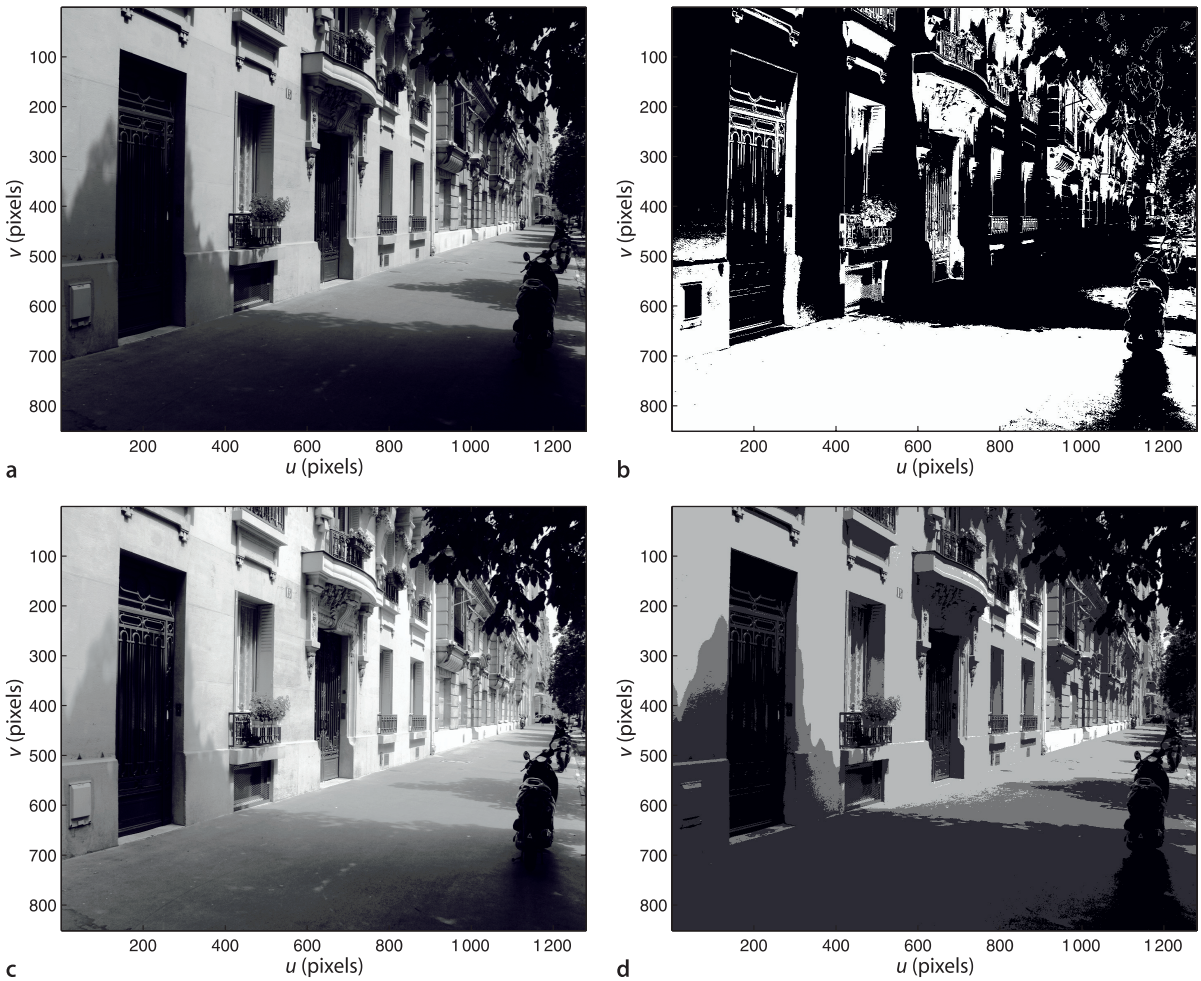

Fig. 12.7. Some monadic image operations, **a** original, **b** shadow regions, **c** histogram normalized, **d** posterization

exposed image will have no low values. We can apply a linear mapping to the grey-scale values

```
>> im = istretch(street);
```

which ensures that pixel values span the full range which is either [0, 1] or [0, 255] depending on the class of the image.

The histogram of such an image will have gaps. If M is the maximum possible pixel value, and $N < M$ is the maximum value in the image then the stretched image will have at most N unique pixel values, meaning that $M - N$ values cannot occur.

A more sophisticated version is histogram normalization or histogram equalization

```
>> im = inormhist(street);
```

which is shown in Fig. 12.7c and ensures that the cumulative distribution of pixel intensities is linear. We see that the grey levels in the shadow region have been raised and stretched out making the details in the shadowed area more visible. The cumulative histogram of the pixel values can be plotted using

```
>> ihist(street, 'cdf');
```

The cumulative distributions of the image before and after normalization are shown in Fig. 12.6b.

> Operations such as `istretch` and `inormhist` can *enhance* the image from the perspective of a human observer, but it is important to remember that no new information has been added to the image. Subsequent image processing steps will not be improved.

As discussed in Sect. 10.3.4 the output of a camera is generally gamma encoded so that the pixel value is a non-linear function L^{γ} of the luminance sensed at the photosite. Such images can be gamma decoded by a non-linear monadic operation

```
>> im = igamma(street, 1/0.45);
```

which raises each pixel to the specified power, or

```
>> im = igamma(street, 'sRGB');
```

to decode images with the sRGB standard gamma encoding. The resulting *linear* image has greylevels, or tristimulus values, which are proportional to the luminance of the original scene.

Another simple non-linear monadic operation is posterization or banding. This pop-art effect is achieved by reducing the number of grey levels

```
>> idisp( street/64 )
```

as shown in Fig. 12.7d. Since integer division is used the resulting image has pixels with values in the range [0, 3] and therefore just four different shades of grey.

12.3 Diadic Operations

Diadic operations are shown schematically in Fig. 12.8. Two input matrices result in a single output matrix, and all three images are of the same size. Each output pixel is a function of the corresponding pixels in the two input images

$$\boldsymbol{O}[u,v] = f\big(\boldsymbol{I}_1[u,v], \boldsymbol{I}_2[u,v]\big), \quad \forall (u,v) \in \boldsymbol{I}_1$$

Examples of useful diadic operations include binary arithmetic operators such as addition, subtraction, element-wise multiplication, or builtin MATLAB® diadic matrix functions such as `max`, `min`, `bitand`, `atan2` etc.

> Subtracting one `uint8` image from another results in another `uint8` image even though the result is potentially negative. MATLAB® quite properly clamps values to the interval [0, 255] so subtracting a larger number from a smaller number will result in zero not a negative value. With addition a result greater than 255 will be set to 255. To remedy this, the images should be first converted to signed integers using the MATLAB® function `cast` or to floating point values using the Toolbox function `idouble`.

We will illustrate diadic operations with two examples. The first example is a technique used on television to allow the image of a person to be superimposed on some background, for example a weather presenter superimposed on a weather map. The

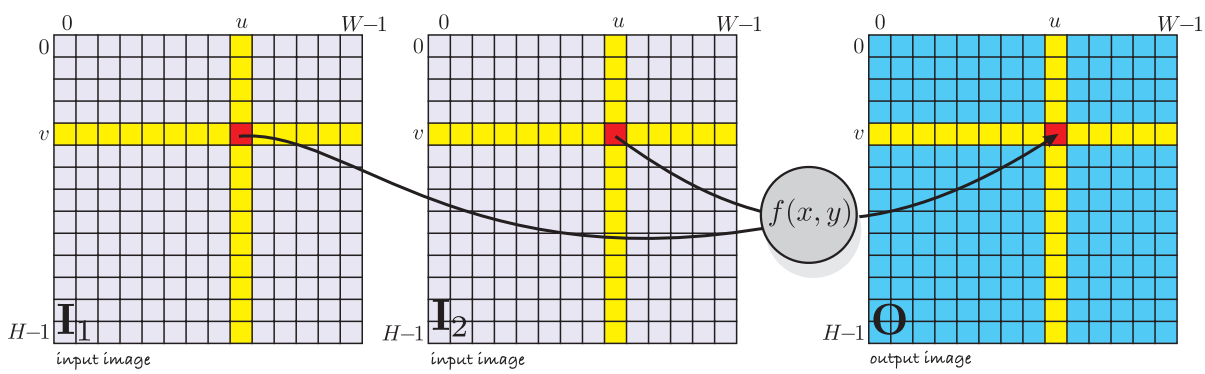

Fig. 12.8. Diadic image processing operations. Each output pixel is a function of the two corresponding input pixels (shown in red)

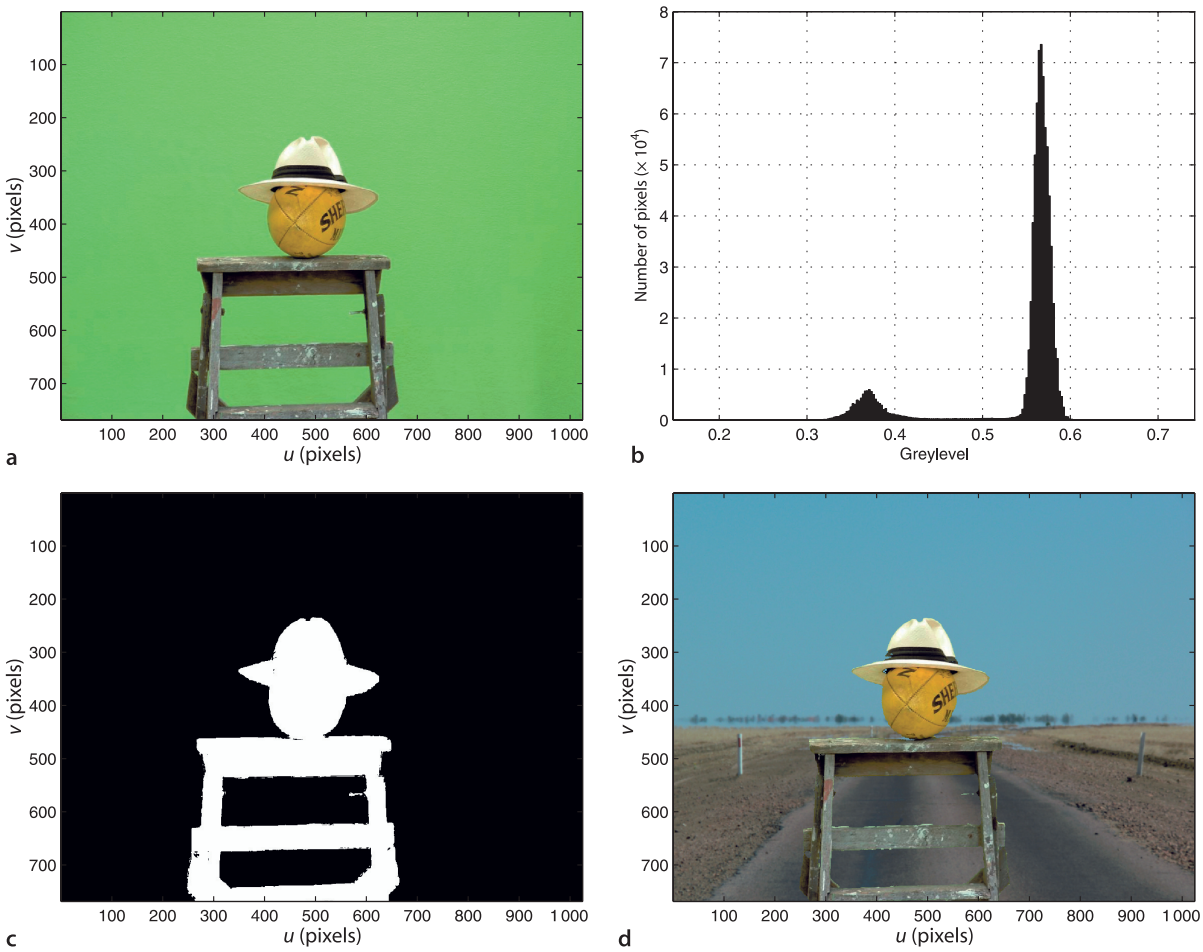

Fig. 12.9. Chroma-keying. **a** The subject against a green background; **b** a histogram of green chromaticity values; **c** the computed mask image where true is white; **d** the subject *masked* into a background scene (photo courtesy of Fiona Corke)

subject is filmed against a blue or green background which makes it quite easy, using just the pixel values, to distinguish between background and the subject. We load an image of a subject taken in front of a green screen

```
>> subject = iread('greenscreen.jpg', 'double');
```

and this is shown in Fig. 12.9a. We compute the chromaticity coordinates Eq. 10.8

```
>> linear = igamma(subject, 'sRGB');
>> [r,g] = tristim2cc(linear);
```

after first converting the gamma encoded color image to linear tristimulus values. In this case g alone is sufficient to distinguish the background pixels. A histogram of values

```
>> ihist(g)
```

shown in Fig. 12.9b indicates a large population of pixels around 0.55 which is the background and another population which belongs to the subject. We can safely say that the subject corresponds to any pixel for which $g < 0.45$. We define a mask image

```
>> mask = g < 0.45;
>> idisp(mask)
```

where a pixel is true (equal to one) if it is part of the subject as shown in Fig. 12.9c. We need to apply this mask to all three so we replicate it

```
>> mask3 = icolor( idouble(mask) );
```

The image of the subject without the background is

```
>> idisp(mask3 .* subject);
```

Next we load the desired background image

```
>> bg = iread('road.png', 'double');
```

and scale and crop it to be the same size as our original image

```
>> bg = isamesize(bg, subject);
```

and display it with a *cutout* for the subject

```
>> idisp(bg .* (1-mask3))
```

Now we add the subject with no background, to the background with no subject to obtain the subject on the road

```
>> idisp( subject.*mask3  + bg.*(1-mask3) );
```

which is shown in Fig. 12.9d. The technique will of course fail if the subject contains any colors that match the color of the background.▶ This example could be solved more compactly using the Toolbox per-pixel switching function `ipixswitch`

In the early days of television a blue screen was used. Today a green background is more popular because of problems that occur with blue eyes and blue denim clothing.

```
>> ipixswitch(mask, subject, bg);
```

where all arguments are images of the same width and height, and each output pixel is selected from the corresponding pixel in the second or third image according to the logical value of the corresponding pixel in the first image.

Distinguishing foreground objects from the background is an important problem in robot vision but the terms foreground and background are ill-defined and application specific. We can be almost guaranteed never to have the luxury of a special background as we did for the chroma-key example. We could instead take a picture of the scene without a foreground object present and consider this to be the background, but that requires that we have special knowledge about when the foreground object is not present. It also assumes that the background does not vary over time. Variation is a significant problem in real-world scenes where ambient illumination and shadows change over quite short time intervals, and the scene may be structurally modified over very long time intervals.

In the next example we process an image sequence and *estimate* the background even though there are a number of objects moving in the scene. We will use a recursive algorithm that updates the estimated background image $\hat{\boldsymbol{B}}$ at each time step based on the previous estimate and the current image

$$\hat{\boldsymbol{B}}\langle k+1\rangle = \hat{\boldsymbol{B}}\langle k\rangle + c\Big(\boldsymbol{I}\langle k\rangle - \hat{\boldsymbol{B}}\langle k\rangle\Big)$$

where k is the time step and $c(\cdot)$ is a monadic image saturation function

$$c(x) = \begin{cases} \sigma, & x > \sigma \\ x, & -\sigma \le x \le \sigma \\ -\sigma, & x < -\sigma \end{cases}$$

To demonstrate this we open a movie showing two people moving in the lobby of a building

```
>> vid = Movie('LeftBag.mpg');
384 x 288 @ 24.999750, 1440 frames
```

and initialize the background to the first image in the sequence

```
>> bg = vid.grab();
```

then the main loop is

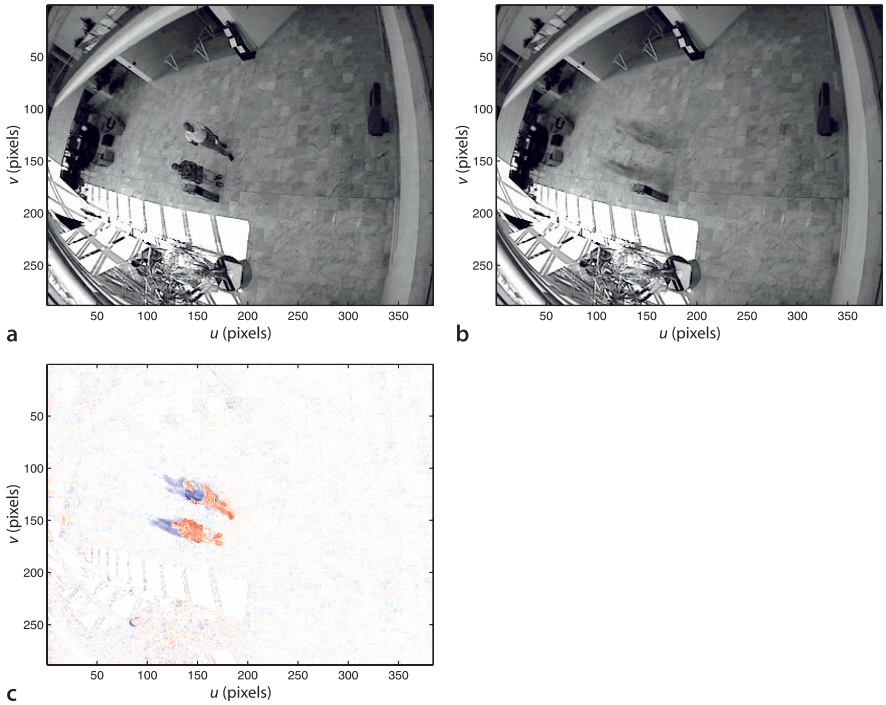

Fig. 12.10. Example of image sequence analysis for the INRIA *LeftBag* image sequence at frame 250. **a** The current image; **b** the estimated background image; **c** the difference between the current and estimated background images where white is zero, red and blue are negative and positive values respectively and magnitude is indicated by color intensity (movie from the collection of the EC Funded CAVIAR project/ IST 2001 37540)

```
sigma = 2;
while 1
   im = vid.grab;
   if isempty(im), break; end
   d = im-bg;
   d = max(min(d, sigma), -sigma);  % apply c(.)
   bg = bg + d;
   idisp(bg);  drawnow
end
```

One frame from this sequence is shown in Fig. 12.10a. The estimated background image shown in Fig. 12.10b reveals the static elements of the scene and the two moving people have become a faint blur. Subtracting the scene from the estimated background creates an image where pixels are bright where they are different to the background as shown in Fig. 12.10c. Applying a threshold to the absolute value of this difference image shows the area of the image where there is motion. Of course if the people stay still long enough they will become part of the background.

12.4 Spatial Operations

Spatial operations are shown schematically in Fig. 12.11. Each pixel in the output image is a function of all pixels in a *region* surrounding the corresponding pixel in the input image

$$\boldsymbol{O}[u,v] = f\big(\boldsymbol{I}[u+i, v+j]\big), \quad \forall (i,j) \in \mathcal{W}, \quad \forall (u,v) \in \boldsymbol{I}$$

where $\mathcal{W}$ is known as the window, typically a $w \times w$ square region with odd side length $w = 2h+1$ where $h \in \mathbb{Z}^+$ is the half-width. In Fig. 12.11 the window includes all pixels in the red shaded region. Spatial operations are powerful because of the variety of possible functions $f(\cdot)$, linear or non-linear, that can be applied. The remainder of this section discusses linear spatial operators such as smoothing and edge detection, and some non-linear functions such as rank filtering and template matching. The following section covers a large and important class of non-linear spatial operators known as mathematical morphology.

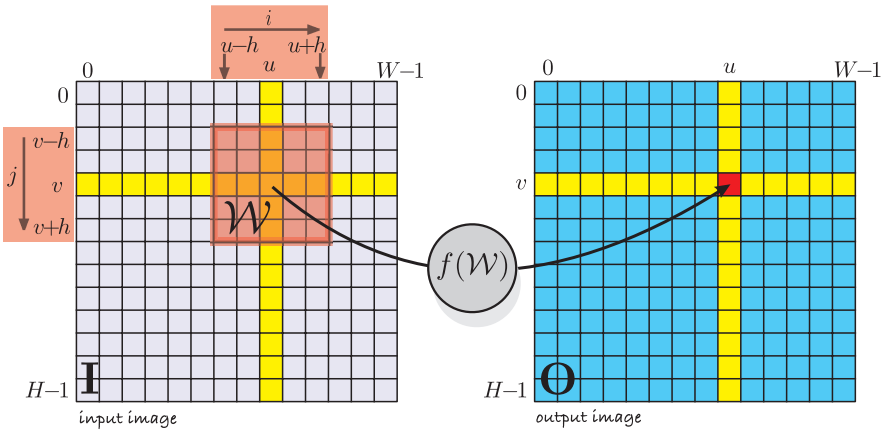

Fig. 12.11.
Spatial image processing operations. The red shaded region shows the window $\mathcal{W}$ that is the set of pixels used to compute the output pixel (show in red)

12.4.1 Convolution

A very important linear spatial operator is convolution

$$\mathbf{O}[u,v] = \sum_{(i,j)\in\mathcal{W}} \boldsymbol{I}[u+i, v+j]\boldsymbol{K}[i,j], \quad \forall (u,v) \in \mathbf{I}$$

where $\boldsymbol{K} \in \mathbb{R}^{w\times w}$ is the convolution kernel. For every output pixel the corresponding window of pixels from the input image $\mathcal{W}$ is multiplied element-wise with the kernel $\boldsymbol{K}$. The centre of the window and kernel is considered to be coordinate (0, 0) and $i, j \in [-h, h]$. This can be considered as the weighted sum of pixels within the window where the weights are defined by the kernel $\boldsymbol{K}$. As we will see convolution is the workhorse of image processing and the kernel $\boldsymbol{K}$ can be chosen to perform functions such as smoothing, gradient calculation or edge detection. Convolution is often written in operator form as

$$\mathbf{O} = K \otimes \mathbf{I}$$

Convolution is computationally expensive – an $N \times N$ input image with a $w \times w$ kernel requires w^2N^2 multiplication and additions. In the Toolbox convolution is performed using the function `iconv`

```
>> O = iconv(K, I);
```

If `I` has multiple color planes then so will the output image – each output color plane is the convolution of the corresponding input plane with the kernel `K`.

Properties of convolution. Convolution obeys the familiar rules of algebra, it is commutative

$$A \otimes B = B \otimes A$$

associative

$$A \otimes B \otimes C = (A \otimes B) \otimes C = A \otimes (B \otimes C)$$

distributive (superposition applies)

$$A \otimes (B + C) = A \otimes B + A \otimes C$$

linear

$$A \otimes (\alpha B) = \alpha(A \otimes B)$$

and shift invariant – if $S(\cdot)$ is a spatial shift then

$$A \otimes S(B) = S(A \otimes B)$$

that is, convolution with a shifted image is the same as shifting the result of the convolution with the unshifted image.

12.4.1.1 Smoothing

Consider a kernel which is a square 21 × 21 matrix containing equal elements

```
>> K = ones(21,21) / 21^2;
```

and of unit volume, that is, its values sum to one. The result of convolving an image with this kernel is an image where each output pixel is the mean of the pixels in a corresponding 21 × 21 neighbourhood in the input image. As you might expect this averaging

```
>> lena = iread('lena.pgm', 'double');
>> idisp( iconv(K, lena) );
```

leads to smoothing, blurring or *defocus*◂ which we see in Fig. 12.12b. Looking very carefully we will see some faint horizontal and vertical lines – an artefact known as ringing. A more suitable kernel for smoothing is the 2-dimensional Gaussian function

Defocus involves a kernel which is a 2-dimensional Airy pattern or sinc function. The Gaussian function is similar in shape, but is always positive whereas the Airy pattern has low amplitude negative going rings.

$$\mathrm{G}(u, v) = \frac{1}{2\pi\sigma^2} e^{-\frac{u^2+v^2}{2\sigma^2}} \tag{12.1}$$

which is symmetric about the origin and the volume under the curve is unity. The spread of the Gaussian is controlled by the standard deviation parameter σ. Applying this kernel to the image

```
>> K = kgauss(5);
>> idisp( iconv(K, lena) );
```

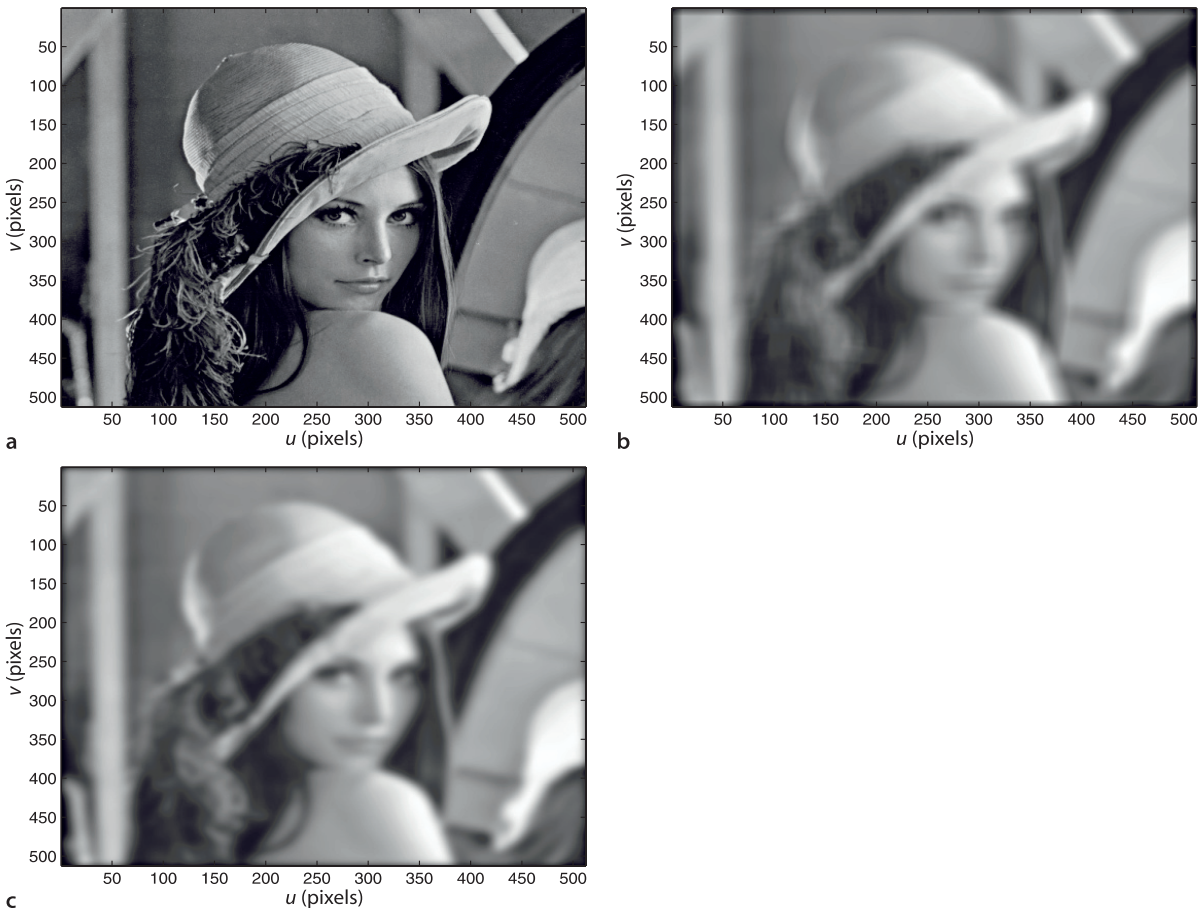

Fig. 12.12. Smoothing. **a** Original image; **b** smoothed with a 21 × 21 averaging kernel; **c** smoothed with a 31 × 31 Gaussian $G(\sigma = 5)$ kernel

The Lena image became something of a standard for image processing research in the 1970s. It was digitized by image compression researchers at the University of Southern California Signal and Image Processing Institute (SIPI) in 1973 from a November 1972 Playboy centerfold. The model is Lena Soderberg (nee Sjööblom) who lives in Sweden. She is reported to be amused by this use of her picture and attended an imaging conference in 1997. See also http://www.lenna.org.

produces the result shown in Fig. 12.12c. Here we have specified the standard deviation of the Gaussian to be 5 pixels. The discrete approximation to the Gaussian is

```
>> about(K)
K [double] : 31x31 (7688 bytes)
```

a 31×31 kernel. Smoothing can be achieved conveniently using the Toolbox function `ismooth`

```
>> idisp( ismooth(lena, 5) )
```

Blurring is a counter-intuitive image processing operation since we typically go to a lot of effort to obtain a clear and crisp image. To deliberately *ruin it* seems, at face value, somewhat reckless. However as we will see Gaussian smoothing turns out to be extremely useful.

The kernel is itself a matrix and therefore we can display it as an image

```
>> idisp( K );
```

which is shown in Fig. 12.13a. We clearly see the large value at the centre of the kernel and that it falls off smoothly in all directions. We can also display the kernel as a surface

```
>> surfl(-15:15, -15:15, K);
```

How wide is my Gaussian? When choosing a Gaussian kernel we need to consider the standard deviation, usually defined by the task, and the dimensions of the kernel $\mathcal{W} \in \mathbb{R}^{w \times w}$ that contains the discrete Gaussian function. Computation time is proportional to w^2 so ideally we want the window to be no bigger than it needs to be. The Gaussian decreases monotonically in all directions but never reaches zero. Therefore we choose the half-width h of the window such that value of the Gaussian is less than some threshold outside the $w \times w$ convolution window.

At the edge of the window, a distance h from the centre, the value of the Gaussian will be $e^{-h^2/2\sigma^2}$. For $\sigma = 1$ and $h = 2$ the Gaussian will be $e^{-2} \approx 0.14$, for $h = 3$ it will be $e^{-4.5} \approx 0.01$, and for $h = 4$ it will be $e^{-8} \approx 3.4 \times 10^{-4}$. If h is not specified the Toolbox chooses $h = 3\sigma$. For $\sigma = 1$ that is a 7×7 window which contains all values of the Gaussian greater than 1% of the peak value.

Properties of the Gaussian. The Gaussian function has some special properties. The convolution of two Gaussians is another Gaussian

$$\mathbf{G}(\sigma_1) \otimes \mathbf{G}(\sigma_2) = \mathbf{G}\left(\sqrt{\sigma_1^2 + \sigma_2^2}\right)$$

For the case where $\sigma_1 = \sigma_2 = \sigma$ then

$$\mathbf{G}(\sigma) \otimes \mathbf{G}(\sigma) = \mathbf{G}\left(\sqrt{2}\sigma\right)$$

The 2-dimensional Gaussian is separable – it can be written as the product of two 1-dimensional Gaussians

$$\mathbf{G}(u, v) = \frac{1}{\sqrt{2\pi}\sigma} e^{\frac{u^2}{2\sigma^2}} \times \frac{1}{\sqrt{2\pi}\sigma} e^{\frac{v^2}{2\sigma^2}}$$

This implies that convolution with a 2-dimensional Gaussian can be computed by convolving each row with a 1-dimensional Gaussian, and then each column. The total number of operations is reduced to $2wN^2$, better by a factor of w. A Gaussian also has the same shape in the spatial and frequency domains.

as shown in Fig. 12.13b. A crude approximation to the Gaussian is the top hat kernel which is cylinder with vertical sides rather than a smooth and gentle fall off in amplitude. The function `kcircle` creates a kernel which can be considered a unit height cylinder of specified radius

```
>> K = kcircle(8, 15);
```

as shown in Fig. 12.13c. The arguments specify a radius of 8 pixels within a window of half width $h = 15$.

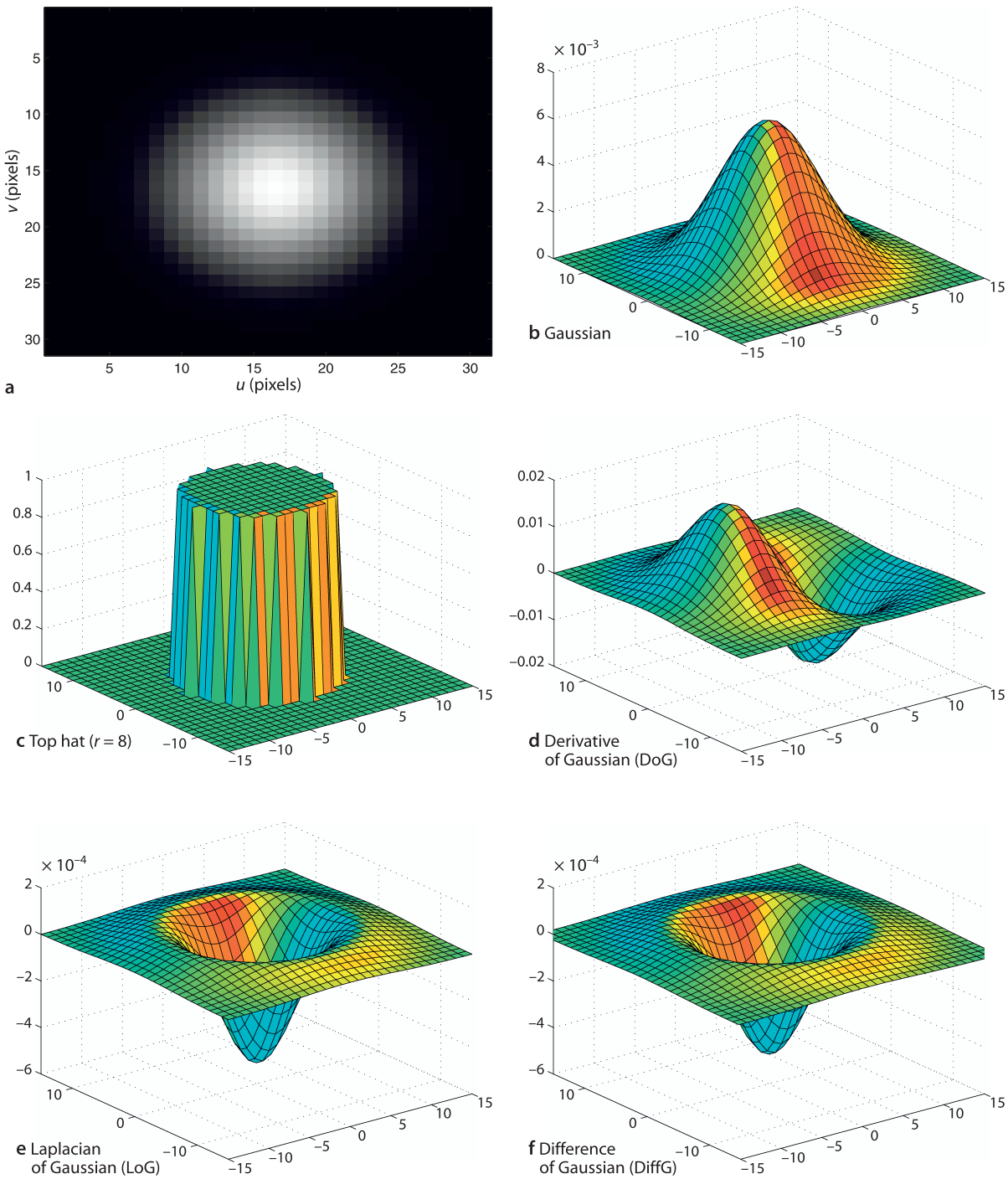

Fig. 12.13. Gallery of commonly used convolution kernels. $h = 15$, $\sigma = 5$

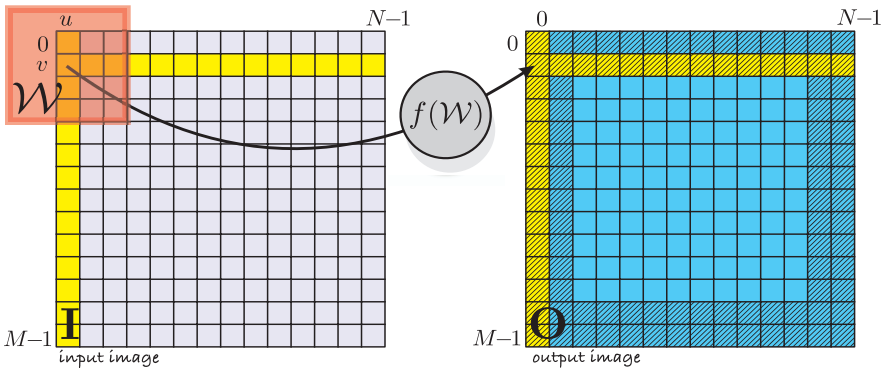

Fig. 12.14.
For the case where the window $\mathcal{W}$ *falls off the edge* of the input image the output pixel at (u, v) is not defined. The hatched pixels in the output image are all those for which the output value is not defined

12.4.1.2 Boundary Effects

A difficulty with convolution occurs when the window is close to the edge of the input image as shown in Fig. 12.14. In this case the output pixel is a function of a window that contains pixels *beyond the edge* of the input image. There are several common remedies to this problem. Firstly, we can assume the pixels beyond the image have a particular value. A common choice is zero and this is the default behaviour implemented by the Toolbox function `iconv`. We can see the effect of this in Fig. 12.12 where the borders of the smoothed image are dark due to the influence of these zeros.

Another option is to consider that the result is invalid when the window exceeds the boundary of the image. Invalid output pixels are shown hatched out in Fig. 12.14. The result is an output image that is $(M - 2h) \times (N - 2h)$. This option can be selected by passing the option `'valid'` to `iconv`.

12.4.1.3 Edge Detection

Frequently we are interested in finding the edges of objects in a scene. Consider the image

```
>> castle = iread('castle_sign.jpg', 'double', 'grey');
```

shown in Fig. 12.15a. It is informative to look at the pixel values along a 1-dimensional profile through the image. A horizontal profile of the image at $v = 360$ is

```
>> p = castle(360,:);
```

which is a vector that we can plot

```
>> plot(p);
```

against the horizontal coordinate u in Fig. 12.15b. The clearly visible tall spikes correspond to the white letters and other markings on the sign. Looking at one of the spikes more closely, Fig. 12.15c, we see the intensity profile across the vertical stem of the letter T. The background intensity ≈ 0.3 and the bright intensity ≈ 0.9 but will depend on lighting levels. However the very rapid increase over the space of just a few pixels is distinctive and a more reliable indication of an edge than any decision based on the actual grey levels.

The first-order derivative along this cross-section is

$$p'[v] = p[v] - p[v-1]$$

which can be computed using the MATLAB® function `diff`

```
>> plot(diff(p))
```

and is shown in Fig. 12.15d. The signal is nominally zero with clear non-zero responses at the edges of an object, in this case the edges of the stem of the letter T.

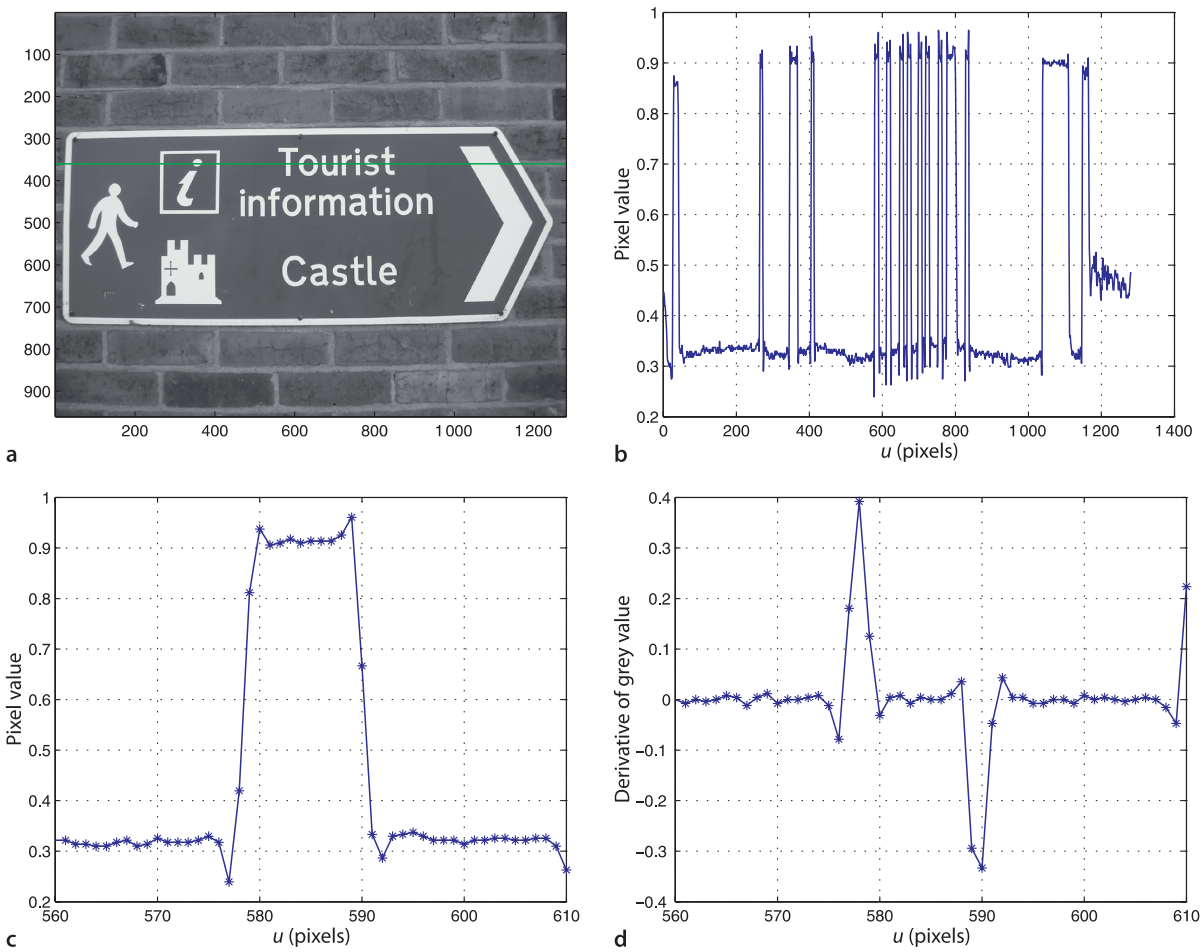

Fig. 12.15. Edge intensity profile. **a** Original image; **b** greylevel profile along horizontal line $v = 360$; **c** close up view of the spike at $u \approx 580$; **d** derivative of **c** (image from the ICDAR 2005 OCR dataset; Lucas 2005)

The derivative at point v can also be written as a *symmetrical* first-order difference

$$p'[v] = \frac{1}{2}\big(p[v+1] - p[v-1]\big)$$

which is equivalent to convolution with the 1-dimensional kernel

$$K = \begin{pmatrix} -\frac{1}{2} & 0 & \frac{1}{2} \end{pmatrix}$$

Convolving the image with this kernel

```
>> K = [-0.5 0 0.5];
>> idisp( iconv(castle, K), 'invsigned')
```

produces a result very similar to that shown in Fig. 12.16a in which vertical edges, high horizontal gradients, are clearly seen.

> Since this kernel has signed values the result of the convolution will also be signed, that is, the gradient at a pixel can be positive or negative as shown in Fig. 12.15d. `idisp` always displays the minimum, most negative, value as black and the maximum, most postive, value as white. Zero would therefore appear as middle grey. The `'signed'` option to `idisp` uses red and blue shading to clearly indicate sign – zero is black, negative pixels are red, positive pixels are blue and the intensity of the color is proportional to pixel magnitude. The `'invsigned'` option is similar except that zero is indicated by white.

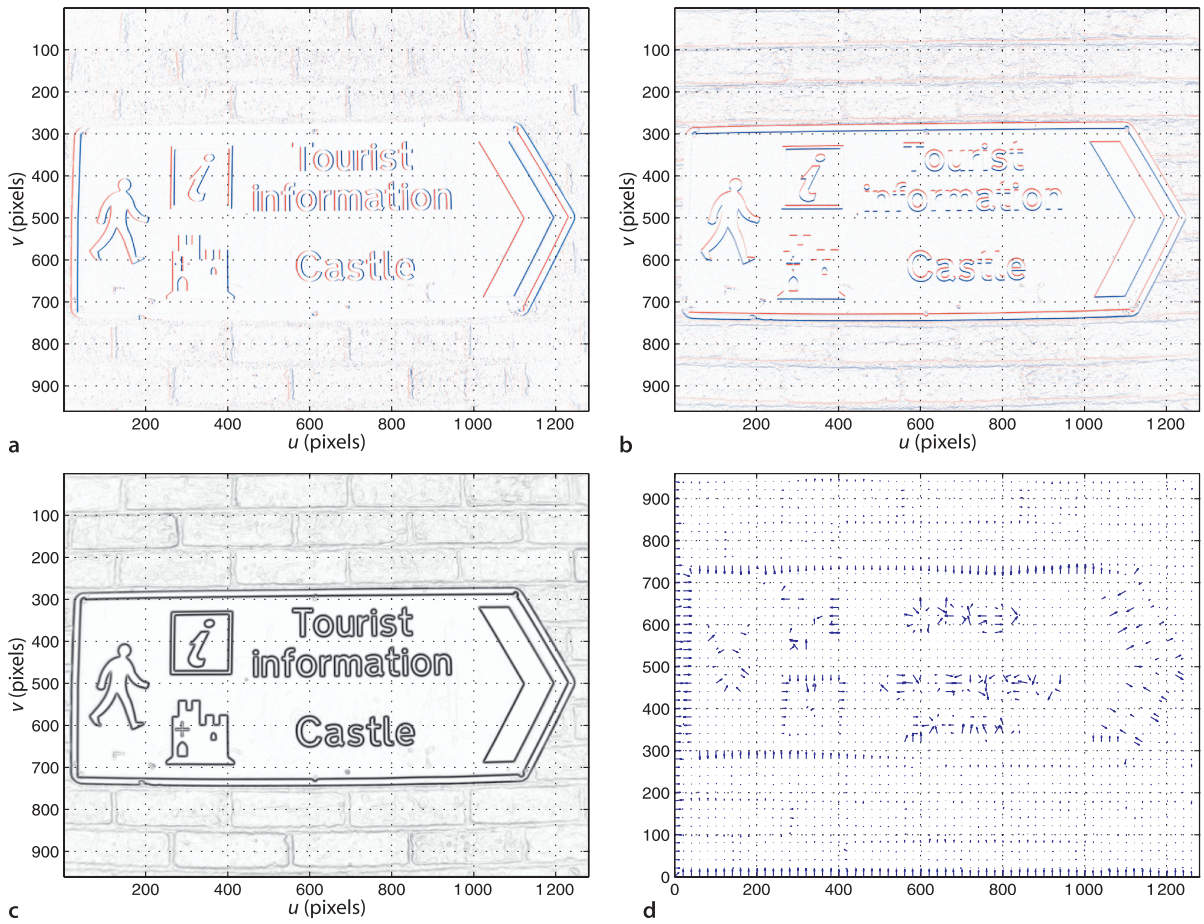

Fig. 12.16. Edge gradient. **a** u-axis derivative; **b** v-axis derivative; **c** gradient magnitude; **d** gradient direction

Many convolution kernels have been proposed for computing horizontal gradient. The most common is the Sobel kernel

```
>> Du = ksobel
Du =
     -1      0      1
     -2      0      2
     -1      0      1
```

and each row is similar to the 1-dimensional kernel `K` defined above. The overall result is a weighted sum of the horizontal gradient for the current row, and the rows above and below. Convolving our image with this kernel

```
>> idisp( iconv(castle, Du), 'invsigned')
```

generates the horizontal gradient image shown in Fig. 12.16a which highlights vertical edges. Vertical gradient is computed using the transpose of the kernel

```
>> idisp( iconv(castle, Du'), 'invsigned')
```

and highlights horizontal edges▸ as shown in Fig. 12.16b. The notation used for gradients varies considerably in the literature. Most commonly the horizontal and vertical gradient are denoted respectively as $\partial \mathbf{I}/\partial u, \partial \mathbf{I}/\partial v$; $\nabla_u \mathbf{I}, \nabla_v \mathbf{I}$ or $\mathbf{I}_u, \mathbf{I}_v$. In operator form this is written

$$\mathbf{I}_u = \mathbf{D} \otimes \mathbf{I}$$
$$\mathbf{I}_v = \mathbf{D}^T \otimes \mathbf{I}$$

where $\mathbf{D}$ is a derivative kernel such as Sobel.

Filters can be designed to respond to edges at any arbitrary angle. The Sobel kernel itself can be considered as an image and rotated using `irotate`. To obtain angular precision generally requires a larger kernel is required such as that generated by `kdgauss`.

Carl Friedrich Gauss (1777–1855) was a German mathematician who made major contributions to fields such as number theory, differential geometry, magnetism, astronomy and optics. He was a child prodigy, born in Brunswick, Germany, the only son of uneducated parents. At the age of three he corrected, in his head, a financial error his father had made, and made his first mathematical discoveries while in his teens.

Gauss was a perfectionist and a hard worker but not a prolific writer. He refused to publish anything he did not consider complete and above criticism. It has been suggested that mathematics could have been advanced by fifty years if he had published all of his discoveries. According to legend Gauss was interrupted in the middle of a problem and told that his wife was dying – he responded "Tell her to wait a moment until I am through".

The normal distribution, or Gaussian function, was not one of his achievements. It was first discovered by de Moivre in 1733 and again by Laplace in 1778.

Taking the derivative of a signal accentuates high-frequency noise, and all images have noise as discussed on page 260. At the pixel level noise is a stationary random process – the values are not cor-related between pixels. However the features that we are interested in such as edges have correlated changes in pixel value over a larger spatial scale as shown in Fig. 12.15c. We can reduce the effect of noise by smoothing the image before taking the derivative

$$\mathbf{I}_u = \mathbf{D} \otimes \big(\mathbf{G}(\sigma) \otimes \mathbf{I}\big)$$

Instead of convolving the image with the Gaussian and *then* the derivative, we exploit the associative property of convolution to write

$$\nabla \mathbf{I} = \mathbf{D} \otimes \big(\mathbf{G}(\sigma) \otimes I\big) = \underbrace{\big(\mathbf{D} \otimes \mathbf{G}(\sigma)\big)}_{\text{DoG}} \otimes \mathbf{I}$$

We convolve the image with the *derivative of the Gaussian* (DoG) which can be obtained numerically by

```
>> Gu = iconv( Du, kgauss(sigma) );
```

or analytically by taking the derivative, in the u-direction, of the Gaussian Eq. 12.1 yielding

$$\mathbf{G}_u(u, v) = -\frac{u}{2\pi\sigma^2} e^{-\frac{u^2+v^2}{2\sigma^2}} \tag{12.2}$$

This is computed by the Toolbox function `kdgauss` and is shown in Fig. 12.13d. The standard deviation σ controls the *scale* of the edges that are detected. For large σ, which implies increased smoothing, edges due to fine texture will be attenuated leaving only the edges of large features. This ability to find edges at different spatial scale is important and underpins the concept of scale space that we will return to in Sect. 13.3.2. Another interpretation of this operator is as a spatial *bandpass filter* since it is a cascade of a low-pass filter (smoothing) with a high-pass filter (differentiation).

Computing the horizontal and vertical components of gradient at each pixel

```
>> Iu = iconv( castle, kdgauss(2) );
>> Iv = iconv( castle, kdgauss(2)' );
```

allows us to compute the magnitude of the gradient at each pixel

```
>> m = sqrt( Iu.^2 + Iv.^2 );
```

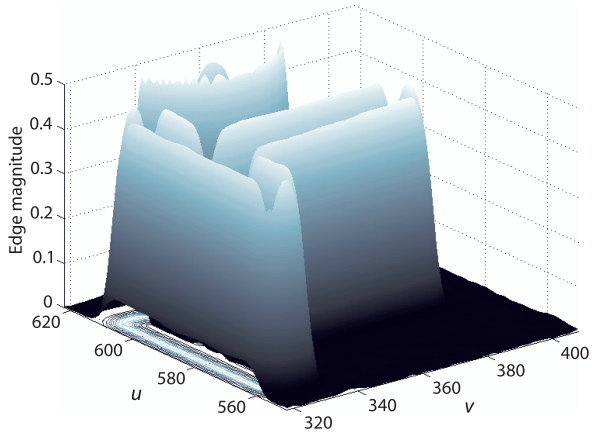

Fig. 12.17.
Close up of gradient magnitude around the letter T shown as a 3-dimensional surface

This *edge-strength* image shown in Fig. 12.16c reveals the edges very distinctly. The direction of the gradient at each pixel is

```
>> th = atan2( Iv, Iu);
```

and is best viewed as a sparse quiver plot

```
>> quiver(1:20:numcols(th), 1:20:numrows(th), ...
        Iu(1:20:end,1:20:end), Iv(1:20:end,1:20:end))
```

as shown in Fig. 12.16d. The edge direction plot is much noisier than the magnitude plot. Where the edge gradient is strong, on the border of the sign or the edges of letters, the direction is normal to the edge, but the fine-scale brick texture appears as almost random edge direction. The gradient images can be computed conveniently using the Toolbox function

```
>> [du,dv] = isobel( castle, kdgauss(2) );
```

where the last argument overrides the default Sobel kernel.

A well known and very effective edge detector is the Canny edge operator. It uses the edge magnitude and direction that we have just computed and performs two additional steps. The first is non-local maxima suppression. Consider the gradient magnitude image of Fig. 12.16c as a 3-dimensional surface where height is proportional to brightness as shown in Fig. 12.17. We see a series of hills and ridges and we wish to find the pixels that lie at the tops of hills or along *ridge lines*. By examining pixel values in a local neighbourhood *normal* to the edge direction, that is in the direction of the edge gradient, we can find the maximum value and set all other pixels to zero. The result is a set of non-zero pixels corresponding to peaks and ridge lines. The second step is hysteresis thresholding. For each non-zero pixel that exceeds the upper threshold a chain is created of adjacent pixels that exceed the lower threshold. Any other pixels are set to zero.

To apply the Canny operator to our example image is straightforward

```
>> edges = icanny(castle, 2);
```

Pierre-Simon Laplace (1749–1827) was a French mathematician and astronomer who consolidated the theories of mathematical astronomy in his five volume *Mécanique Céleste* (Celestial Mechanics). While a teenager his mathematical ability impressed d'Alembert who helped to procure him a professorship. When asked by Napoleon why he hadn't mentioned God in his book on astronomy he is reported to have said "Je n'avais pas besoin de cette hypothèse-là" ("I have no need of that hypothesis"). He became a count of the Empire in 1806 and later a marquis.

The Laplacian operator, a second-order differential operator, and the Laplace transform are named after him.

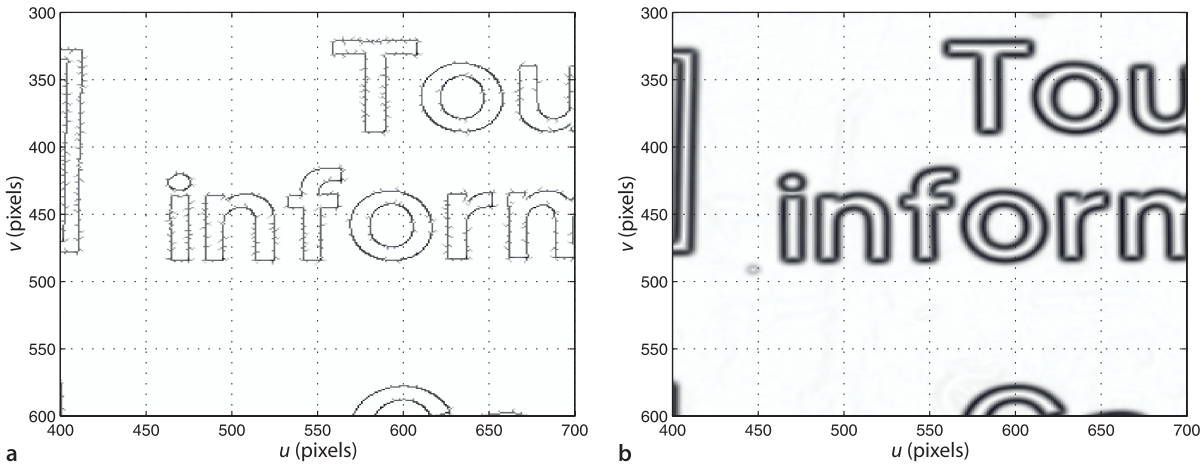

Fig. 12.18. Comparison of two edge operators: **a** Canny operator with default parameters; **b** Magnitude of derivative of Gaussian kernel ($\sigma = 2$). The |DoG| operator requires less computation than Canny but generates thicker edges. For both cases results are shown inverted, white is zero

and returns an image where the edges are marked by non-zero intensity values corresponding to gradient magnitude at that pixel as shown in Fig. 12.18a. We observe that the edges are much thinner than those for the magnitude of derivative of Gaussian operator which is shown in Fig. 12.18b. In this example $\sigma = 2$ for the derivative of Gaussian operation. The hysteresis threshold parameters can be set with optional arguments.

So far we have considered an edge as a point of high gradient, and non-maxima suppression has been used to *search* for the maximum value in local neighbourhoods. An alternative means to find the point of maximum gradient is to compute the second derivative and determine where this is zero. The Laplacian operator

$$\nabla^2 \mathbf{I} = \frac{\partial^2 \mathbf{I}}{\partial u^2} + \frac{\partial^2 \mathbf{I}}{\partial v^2} = \mathbf{I}_{uu} + \mathbf{I}_{vv} \tag{12.3}$$

is the sum of the second spatial derivative in the horizontal and vertical directions. For a discrete image this can be computed by convolution with the Laplacian kernel

```
>> L = klaplace()
L =
     0     1     0
     1    -4     1
     0     1     0
```

which is isotropic – it responds equally to edges in any direction. The second derivative is even more sensitive to noise than the first derivative and is again commonly used in conjunction with a Gaussian smoothed image

$$\nabla^2 \mathbf{I} = \mathbf{L} \otimes \big(\mathbf{G}(\sigma) \otimes \mathbf{I}\big) = \underbrace{\big(\mathbf{L} \otimes \mathbf{G}(\sigma)\big)}_{\text{LoG}} \otimes \mathbf{I} \tag{12.4}$$

which we combine into the Laplacian of Gaussian kernel (LoG), and $\mathbf{L}$ is the Laplacian kernel given above. This can be written analytically as

$$\mathbf{LoG}(u, v) = \frac{\partial^2 \mathbf{G}}{\partial u^2} + \frac{\partial^2 \mathbf{G}}{\partial v^2} \tag{12.5}$$

$$= \frac{1}{\pi \sigma^4} \left(\frac{u^2 + v^2}{2\sigma^2} - 1 \right) e^{-\frac{u^2+v^2}{2\sigma^2}} \tag{12.6}$$

which is known as the Marr-Hildreth operator or the *Mexican hat kernel* and is shown in Fig. 12.13e.

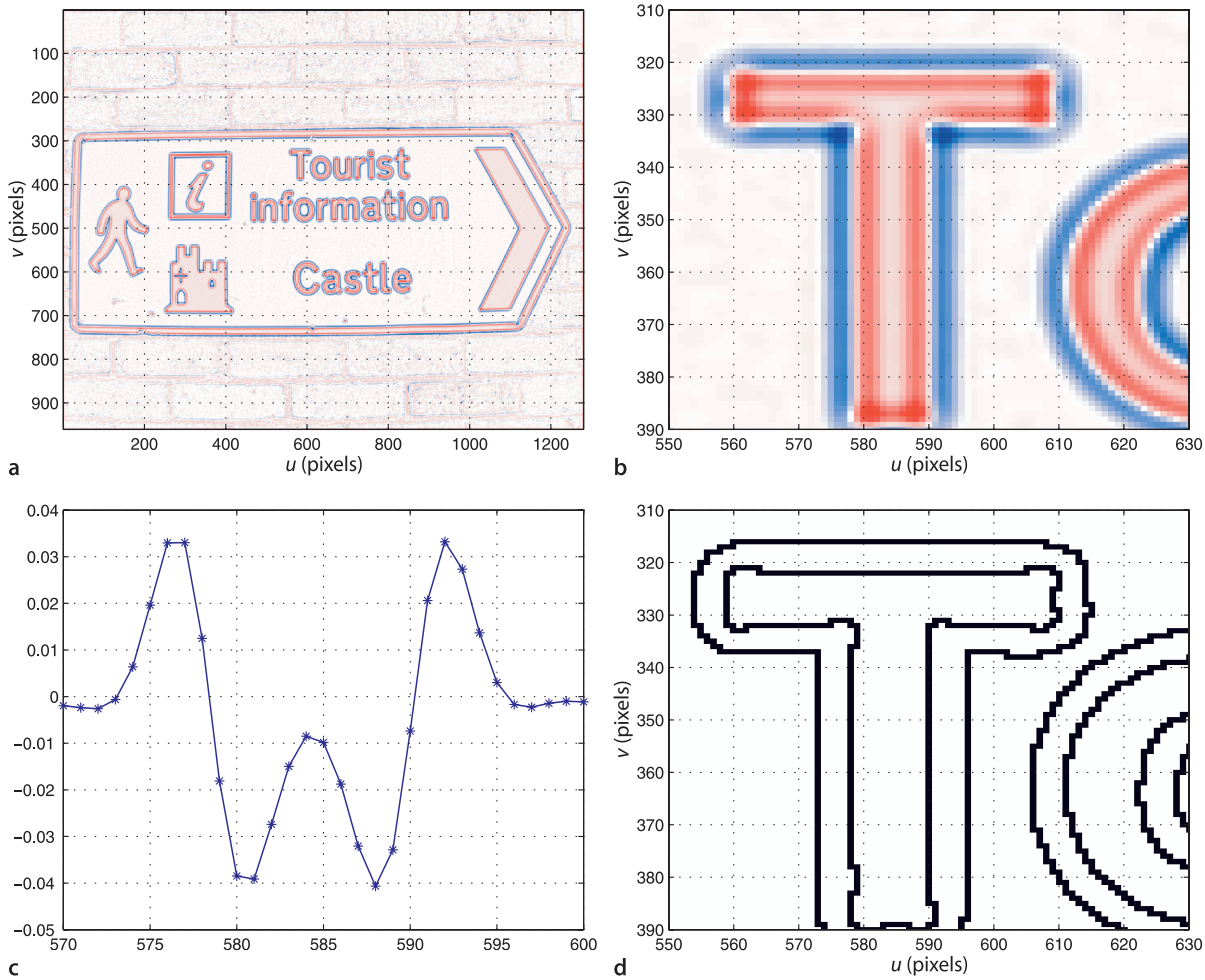

Fig. 12.19. Laplacian of Gaussian. **a** Laplacian of Gaussian; **b** closeup of **a** around the letter T where blue and red colors indicate positive and negative values respectively; **c** a horizontal cross-section of the LoG through the stem of the T; **d** closeup of the zero-crossing detector output at the letter T

We apply this kernel to our image by

```
>> lap = iconv( castle, klog(2) );
```

and the result is shown in Fig. 12.19a and b. The maximum gradient occurs where the second derivative is zero but a significant edge is a zero crossing from a strong positive value (blue) to a strong negative value (red). Consider the closeup view of the Laplacian of the letter T shown in Fig. 12.19b. We generate a horizontal cross-section of the stem of the letter T at $v = 360$

Difference of Gaussians. The Laplacian of Gaussian can be approximated by the difference of two Gaussian functions

$$\mathbf{DiffG}(u, v; \sigma_1, \sigma_1) = \mathbf{G}(\sigma_1) - \mathbf{G}(\sigma_2) = \frac{1}{2\pi\sigma_1^2\sigma_2^2}\left(\sigma_2^2 e^{\frac{u^2+v^2}{2\sigma_1^2}} - \sigma_1^2 e^{\frac{u^2+v^2}{2\sigma_2^2}}\right)$$

where $\sigma_1 > \sigma_2$ and commonly $\sigma_1 = 1.6\sigma_2$. Figure 12.13e and f compares the LoG and DiffG kernels respectively.

This approximation is useful in scale-space sequences which will be discussed in Sect. 13.3.2. Consider an image sequence $\mathbf{I}\langle k\rangle$ where $\mathbf{I}\langle k+1\rangle = \mathbf{G}(\sigma) \otimes \mathbf{I}\langle k\rangle$, that is, the images are increasingly smoothed. The difference between any two images in the sequence is therefore equivalent to $\mathrm{DiffG}(\sqrt{2}\,\sigma, \sigma)$ applied to the original image.

```
>> p = lap(360,570:600);
>> plot(570:600, p, '-*');
```

which is shown in Fig. 12.19c. We see that the zero values of the second derivative lies *between* the pixels. A zero crossing detector selects pixels adjacent to the zero crossing points

```
>> zc = zcross(lap);
```

and this is shown in Fig. 12.19d. We see that the edges appear twice. Referring again to Fig. 12.19c we observe a weak zero crossing in the interval $u \in [573, 574]$ and a much more definitive zero crossing in the interval $u \in [578, 579]$.

A fundamental limitation of all edge detection approaches is that intensity edges do not necessarily delineate the boundaries of objects. The object may have poor contrast with the background which results in weak boundary edges. Conversely the object may have a stripe on it which is not its edge. Shadows frequently have very sharp edges but are not real objects. Object texture will result in a strong output from an edge detector at points not just on its boundary, as for example with the bricks in Fig. 12.15b.

12.4.2 Template Matching

In our discussion so far we have used kernels that represent mathematical functions such as the Gaussian and its derivative and its Laplacian. We have also considered the convolution kernel as a matrix, a 3-dimensional shape and even an image as shown in Fig. 12.13a. In this section we will consider that the kernel *is an image* or a part of an image and such a kernel is referred to as a template. In template matching we wish to find which parts of the input image are most similar to the template.

Template matching is shown schematically in Fig. 12.20. Each pixel in the output image is given by

$$\mathbf{O}[u, v] = s(\mathbf{T}, \mathcal{W}), \quad \forall (u, v) \in \mathbf{I}$$

where $\mathbf{T}$ is the $w \times w$ template, the pattern of pixels we are looking for, with odd side length $w = 2h + 1$, and $\mathcal{W}$ is the $w \times w$ window centred at (u, v) in the input image. The function $s(\mathbf{I}_1, \mathbf{I}_2)$ is a scalar measure that describes the *similarity* of two equally sized images $\mathbf{I}_1$ and $\mathbf{I}_2$.

These measures can be augmented with a Gaussian weighting to deemphasize the differences that occur at the edges of the two windows.

A number of common similarity measures◂ are given in Table 12.1. The most intuitive are computed simply by computing the pixel-wise difference $\boldsymbol{T} - \mathcal{W}$ and taking

David Marr (1945–1980) was a British neuroscientist and psychologist who synthesized results from psychology, artificial intelligence, and neurophysiology to create the discipline of Computational Neuroscience. He studied mathematics at Trinity College, Cambridge and his PhD in physiology was concerned with modeling the function of the cerebellum. His key results were published in three journal papers between 1969 and 1971 and formed a theory of the function of the mammalian brain much of which remains relevant today. In 1973 he was a visiting scientist in the Artificial Intelligence Laboratory at MIT and later became a professor in the Department of Psychology. His attention shifted to the study of vision and in particular the so-called early visual system.

He died of leukemia at age 35 and his book *Vision: A computational investigation into the human representation and processing of visual information* (Marr 2010) was published after his death.

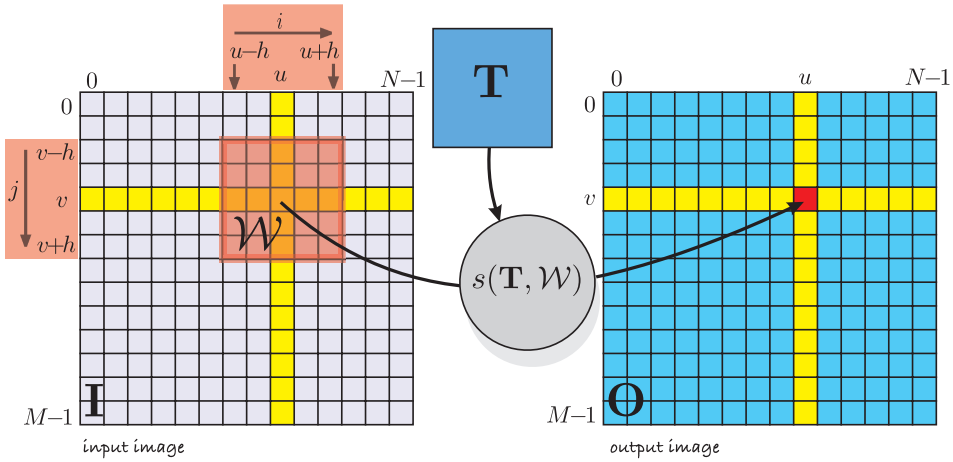

Fig. 12.20.
Spatial image processing operations. The red shaded region shows the window $\mathcal{W}$ that is the set of pixels used to compute the output pixel (shown in red)

Sum of absolute differences		
SAD	$s = \sum_{(u,v)\in I} \lvert I_1[u,v] - I_2[u,v] \rvert$	`sad`
ZSAD	$s = \sum_{(u,v)\in I} \lvert (I_1[u,v] - \bar{I}_1) - (I_2[u,v] - \bar{I}_2) \rvert$	`zsad`
Sum of squared differences		
SSD	$s = \sum_{(u,v)\in I} (I_1[u,v] - I_2[u,v])^2$	`ssd`
ZSSD	$s = \sum_{(u,v)\in I} ((I_1[u,v] - \bar{I}_1) - (I_2[u,v] - \bar{I}_2))^2$	`zssd`
Cross correlation		
NCC	$s = \frac{\sum_{(u,v)\in I} I_1[u,v] \cdot I_2[u,v]}{\sqrt{\sum_{(u,v)\in I} I_1^2[u,v] \cdot \sum_{(u,v)\in I} I_2^2[u,v]}}$	`ncc`
ZNCC	$s = \frac{\sum_{(u,v)\in I} (I_1[u,v] - \bar{I}_1) \cdot (I_2[u,v] - \bar{I}_2)}{\sqrt{\sum_{(u,v)\in I} (I_1[u,v] - \bar{I}_1)^2 \cdot \sum_{(u,v)\in I} (I_2[u,v] - \bar{I}_2)^2}}$	`zncc`

Table 12.1.
Similarity measures for two equal-sized image regions I_1 and I_2. The Z-prefix indicates that the measure accounts for zero-offset or the difference in mean of the two images (Banks and Corke 2001). $\bar{I}_1$ and $\bar{I}_2$ are the mean of image regions I_1 and I_2 respectively. Toolbox functions are indicated in the last column

the sum of the absolute differences (SAD) or the sum of the squared differences (SSD). These metrics are zero if the images are identical and increase with dissimilarity. It is not easy to say what value of the measure constitutes a poor match but a ranking of similarity measures can be used to determine the *best* match.

More complex measures such as normalized cross-correlation yield a score in the interval $[-1, +1]$ with $+1$ for identical regions. In practice a value greater than 0.8 is considered to be a good match. Normalized cross correlation is however computationally more expensive – requiring multiplication, division and square root operations. Note that it is possible for the result to be undefined if the denominator is zero, which occurs if the the elements of either I_1 or I_2 are identical.

If $I_2 \equiv I_1$ then it is easily shown that SAD = SSD = 0 and NCC = 1 indicating a perfect match. To illustrate we will create a 51×51 template

```
>> T = iroi(lena, [240 290; 250 300]);
```

and evaluate the three common measures

```
>> sad(T, T)
ans =
     0
>> ssd(T, T)
ans =
     0
>> ncc(T, T)
ans =
     1
```

Now consider the case where the two images are of the same scene but one image is darker than the other – the illumination or the camera exposure has changed. In this case $\boldsymbol{I}_2 = \alpha \boldsymbol{I}_1$ and now

```
>> sad(T, T*0.9)
ans =
  132.8090
>> ssd(T, T*0.9)
ans =
    7.3307
```

these measure indicate a high degree of disimilarity. However the normalized cross-correlation

```
 >> ncc(T, T*0.9)
ans =
     1
```

is invariant to the change in intensity.

This could be due to an incorrect black level setting. A camera's black level is the value of a pixel corresponding to no light and is often >0.

Next consider that the pixel values are also offset so that $I_2 = \alpha I_1 + \beta$ and we find that

```
>> sad(T, T+0.1)
ans =
  260.1000
>> ssd(T, T+0.1)
ans =
   26.0100
>> ncc(T, T+0.1)
ans =
    0.9990
```

all measures indicate a degree of disimilarity. The problematic offset can be dealt with by first subtracting from each of $\mathbf{T}$ and $\mathcal{W}$ their mean value

```
>> zsad(T, T+0.1)
ans =
   1.7300e-11
>> zssd(T, T+0.1)
ans =
   1.1507e-25
>> zncc(T, T+0.1)
ans =
    1.0000
```

and these measures indicate a high degree of similarity. The z-prefix denotes variants of the similarity measures described above that are invariant to intensity offset. Only the ZNCC measure

```
>> zncc(T, T*0.9+0.1)
ans =
    1.0000
```

is invariant to both gain and offset variation. All these methods will fail if the images have even a small change in relative rotation or scale.

Consider the problem from the well known children's book "Where's Wally" or "Where's Waldo" – the fun is trying to find Wally's face in a crowd

```
>> crowd = iread('wheres-wally.png', 'double');
>> idisp(crowd)
```

Fortunately we know roughly what he looks like and the template

```
>> T = iread('wally.png', 'double');
>> idisp(T)
```

was extracted from a different image and scaled so that the head is approximately the same width as other heads in the crowd scene (around 21 pixel wide).

The similarity of our template `T` to every possible window location is computed by

```
>> S = isimilarity(T, crowd, @zncc);
```

using the matching measure ZNCC. The result

```
>> idisp(S, 'colormap', 'jet', 'bar')
```

is shown in Fig. 12.21 and the pixel color indicates the ZNCC similarity as indicated by the color bar. We can see a number of spots of high similarity (red) which are candidate positions for Wally. The peak values, with respect to a local 3×3 window, are

```
>> [mx,p] = peak2(S, 1, 'npeaks', 5);
>> mx
mx =
    0.5258
    0.5230
    0.5222
    0.5032
    0.5023
```

in descending order. The second argument specifies the window half-width $h = 1$ and the third argument specifies the number of features to return. The largest value 0.5258 is the similarity of the strongest match found. These matches occur at the coordinates (u, v) given by the first return value `p` and we can highlight these points on the scene

```
>> idisp(crowd);
>> plot_circle(p, 30, 'fillcolor', 'b', 'alpha', 0.3, 'edgecolor', 'none')
>> plot_point(p, 'sequence', 'bold', 'textsize', 24, 'textcolor', 'k')
```

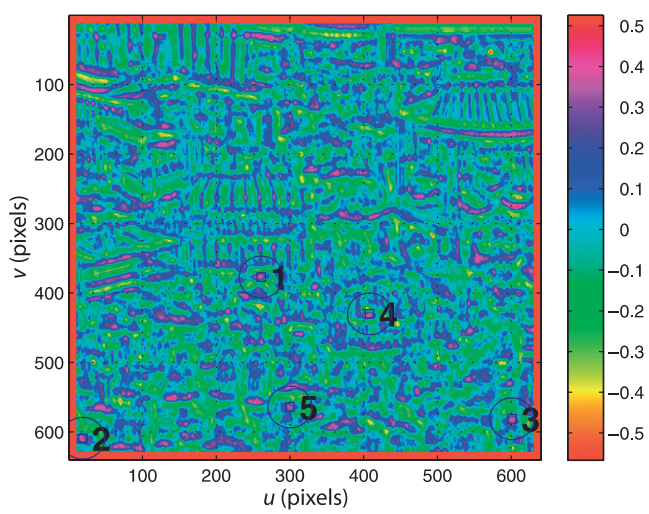

Fig. 12.21.
Similarity image `S` with top five Wally candidates marked. The color bar indicate the similarity scale. Note the border of indeterminate values where the template window falls off the edge of the input image

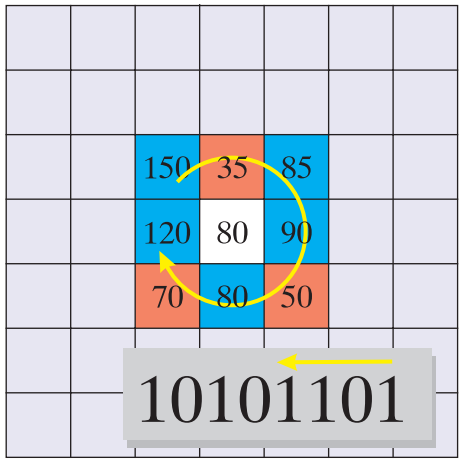

Fig. 12.22. Example of census and rank transform for a 3×3 window. Pixels are marked red or blue if they are less than or greater than or equal to the centre pixel respectively. These boolean values are then packed into a binary word, in the direction shown, from least significant bit upwards. The census value is 10101101_2 or decimal 173. The rank transform value is the total number of one bits and is 5

using transparent blue circles that are numbered sequentially. The best match at (261, 377) is in fact the correct answer – we found Wally! It is interesting to look at the other highly ranked candidates. Numbers two and three at the bottom of the image are people also wearing baseball caps who look quite similar.

There are some important points to note from this example. The images have quite low resolution and the template is only 21×25 – it is a very crude likeness to Wally. The match is not a strong one – only 0.5258 compared to the maximum possible value of 1.0 and there are several contributing factors. The matching measure is not invariant to scale, that is, as the relative scale (zoom) changes the similarity score falls quite quickly. In practice perhaps a 10–20% change in scale between $\mathbf{T}$ and $\mathcal{W}$ can be tolerated. For this example the template was only approximately scaled. Secondly, not all Wallys are the same. Wally in the template is facing forward but the Wally we found in the image is looking to our left. Another problem is that the square template typically includes pixels from the background as well as the object of interest. As the object moves the background pixels may change, leading to a lower similarity score. This is known as the mixed pixel problem. Ideally the template should bound the object of interest as tightly as possible. In practice another problem arises due to perspective distortion. A square pattern of pixels in the centre of the image will appear keystone shaped at the edge of the image and thus will match less well with the square template.

Non-parametric similarity measures are more robust to the mixed pixel problem. Two common measures from this class are the census metric and the rank transform. For the census metric each window, template and candidate, is mapped to a bit string, and each bit corresponds to one pixel in that window as shown in Fig. 12.22. If a pixel is greater than the centre pixel its corresponding bit is set to one, else it is zero. For a $w \times w$ window the string will be $w^2 - 1$ bits long.◀ The two bit strings are compared using a Hamming distance which is the number of bits that are different. This can be computed by counting the number of set bits in the exclusive-or of the two bit strings. Thus very few arithmetic operations are required compared to the more conventional methods – no square roots or division – and such algorithms are amenable to implementation in special purpose hardware or FPGAs. Another advantage is that intensities are considered relative to the centre pixel of the window making it invariant to overall changes in intensity or gradual intensity gradients.

For a 32-bit integer `uint32` this limits the window to 5×5 unless a sparse mapping is adopted (Humenberger et al. 2009). A 64-bit integer `uint64` supports a 7×7 window.

The rank transform maps each window to a scalar which is the number of elements in the window that are greater than the centre pixel. This measure captures the essence of the region surrounding the centre pixel, and like the census measure it is invariant to overall changes in intensity since it is based on local relative grey scale

values. The rank transform is typically used as a pre-processing step applied to each of the images before using a simple classical similarity measure such as SAD. The Toolbox function `isimilarity` supports these metrics using the `'census'` and `'rank'` options.

A common problem with template matching is that false matches can occur. In the example above the second candidate had a similarity score only 0.5% lower than the first, the fifth candidate was only than 5% lower. In practice a number of rules are applied before a match is accepted: the similarity must exceed some threshold and the first candidate must exceed the second candidate by some factor. Another approach is to bring more information to bear on the problem such as known motion of the camera or object. For example if we were tracking Wally from frame to frame in an image sequence then we would pick the best Wally closest to the previous location he was found. Alternatively we could create a motion model and assume he moves approximately the same distance and direction between successive frames. Then we would predict his future position and pick the Wally closest to that predicted position. However we would have to deal with practical difficulties such as Wally stopping, changing direction or becoming obscured.

12.4.3 Non-Linear Operations

Another class of spatial operations is based on non-linear functions of pixels within the window. For example

```
>> out = iwindow(lena, 3, 'var');
```

computes the variance of the pixels in *every* 7×7 window. The arguments specify the window half-width $h = 3$ and the builtin MATLAB® function `var`. The function is called with a 49×1 vector argument comprising the pixels in the window arranged as a column vector and the function's return value becomes the corresponding output pixel value. This operation acts as an edge detector since it has a low value for homogeneous regions irrespective of their brightness. It is however computationally expensive because the `var` function is called over 260 000 times. Any MATLAB® function, builtin or your own M-file, that accepts a vector input and returns a scalar can be used in this way.

Rank filters sort the pixels within the window by value and return the specified element from the sorted list. The maximum value over a 5×5 window about each pixel is the first ranked pixel in the window

```
>> mx = irank(lena, 1, 2);
```

where the arguments are the rank and the window half-width $h = 2$. The median over a 5×5 window is the twelfth in rank

```
>> med = irank(lena, 12, 2);
```

and is useful as a filter to remove impulse-type noise. We can demonstrate this by adding impulse noise to a copy of an image

```
>> spotty = lena;
>> npix = prod(size(lena));
>> spotty(round(rand(5000,1)*(npix-1)+1)) = 0;
>> spotty(round(rand(5000,1)*(npix-1)+1)) = 1.0;
>> idisp(spotty)
```

and this is shown in Fig. 12.23a. We have set 5 000 random pixels to be zero, and another 5 000 random pixels to the maximum value. This type of noise is often referred to as impulse noise or salt and pepper noise. We apply a 3×3 median filter

```
>> idisp( irank(spotty, 5, 1) )
```

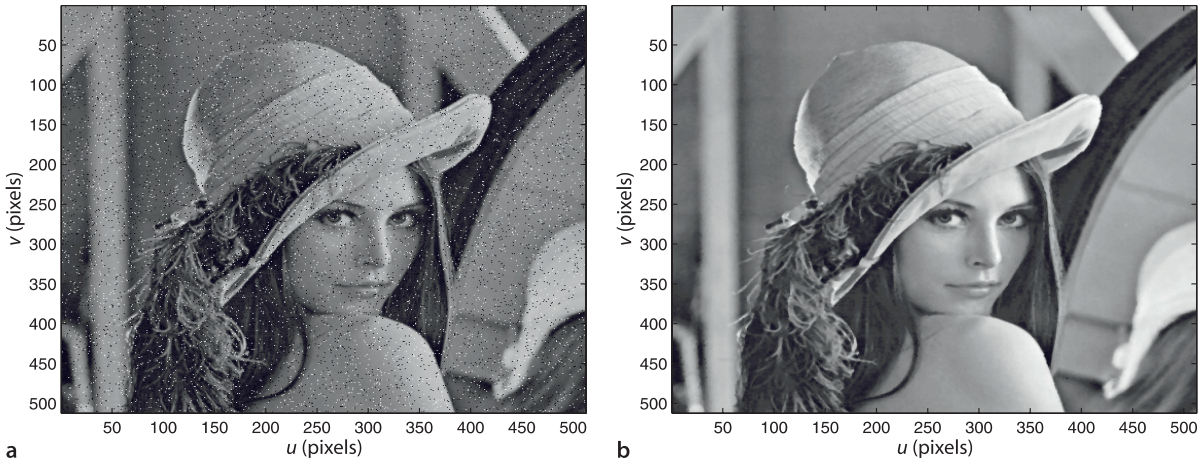

Fig. 12.23. Median filter cleanup of impulse noise. **a** Corrupted image; **b** median filtered result

and the result shown in Fig. 12.23b is considerably improved. A similar effect could have been obtained by smoothing but that would tend to blur the image, median filtering has the advantage of preserving edges in the scene.

The third argument to `irank` can be a matrix instead of a scalar and this allows for some very powerful operations. For example

```
>> M = ones(3,3);
>> M(2,2) = 0
M =
     1     1     1
     1     0     1
     1     1     1
>> mxn = irank(lena, 1, M);
```

specifies the first in rank (maximum) over a *subset* of pixels from the window corresponding to the non-zero elements of `M`. In this case `M` specifies the eight neighbouring pixels but not the centre pixel. The result `mxn` is the maximum of the eight neighbours of each corresponding pixel in the input image. We can use this

```
>> idisp(lena > mxn)
```

to display all those points where the pixel value is greater than its local neighbours and performs non-local maxima suppression. These correspond to local maxima, or peaks if the image is considered as a surface. This mask matrix is very similar to a structuring element which we will meet in the next section.

12.5 Mathematical Morphology

Mathematical morphology is a class of non-linear spatial operators shown schematically in Fig. 12.24. Each pixel in the output matrix is a function of a *subset* of pixels in a region surrounding the corresponding pixel in the input image

$$\mathbf{O}[u,v] = f\big(\mathbf{I}[u+i, v+j]\big), \quad \forall (i,j) \in \mathbb{S}, \quad \forall (u,v) \in \mathbf{I} \tag{12.7}$$

where $\mathbb{S}$ is the structuring element, typically a $w \times w$ square region with odd side length $w = 2h + 1$ where $h \in \mathbb{Z}^+$ is the half-width. The structuring element is similar to the convolution kernel discussed previously except that the function $f(\cdot)$ is applied only to a specified subset of pixels within the window. The selected pixels are those for which the corresponding values of the structuring element are non-zero – these are shown in red in Fig. 12.24. Mathematical morphology, as its name implies, is concerned with the form or *shape* of objects in the image.

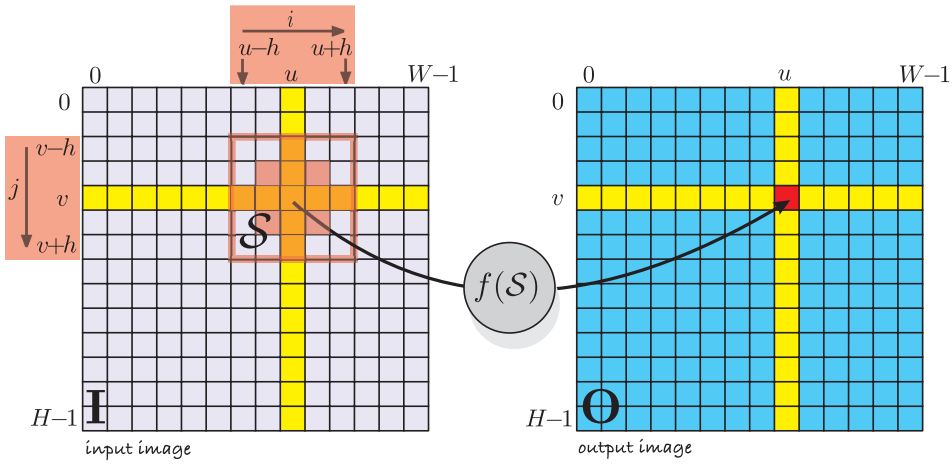

Fig. 12.24.
Morphological image processing operations. The operation is defined only for the selected elements (red) within the structuring element (red outlined square)

The easiest way to explain the concept is with a simple example, in this case a synthetic binary image created by the script

```
>> eg_morph1
>> idisp(im)
```

which is shown, repeated, down the column of Fig. 12.25. The structuring element is shown in red at the end of each row. If we consider the top most row, the structuring element is a square

```
>> S = ones(5,5);
```

and is applied to the original image using the minimum operation

```
>> mn = imorph(im, S, 'min');
```

and the result is shown in the second column. For each pixel in the input image we take the *minimum* of all pixels in the 5×5 window. If *any* of those neighbours is zero the resulting pixel will be zero. The result is dramatic – two objects have disappeared entirely and the two squares have become separated and smaller. The two objects that disappeared were not *consistent* with the shape of the structuring element. This is where the connection to morphology or shape comes in – only shapes that could *contain* the structuring element will be present in the output image.

The structuring element could define a circle, an annulus, a 5-pointed star, a line segment 20 pixels long at 30° to the horizontal or a duck – the technique allows very powerful shape-based filters to be created. The second row shows the results for a larger square structuring element which has resulted in the complete elimination of the small square and the further reduction of the large square. The third row shows the results for a structuring element which is a horizontal line segment 14 pixel wide, and the only remaining shape is the long horizontal line.

The operation we just performed is often known as erosion since large objects are eroded or become smaller – in this case the 5×5 structuring element has caused two pixels▸ to be *shaved off* all the way around the perimeter of each shape. The small square, originally 5×5, is now only 1×1. If we repeated the operation the small square would disappear entirely, and the large square would be reduced even further.

▸ The half width of the structuring element.

The inverse operation is dilation which makes objects larger. In Fig. 12.25 we apply dilation to the second column results

```
>> mx = imorph(mn, S, 'max');
```

and the results are shown in the third column. For each pixel in the input image we take the *maximum* of all pixels in the 5×5 window. If *any* of those neighbours is one the

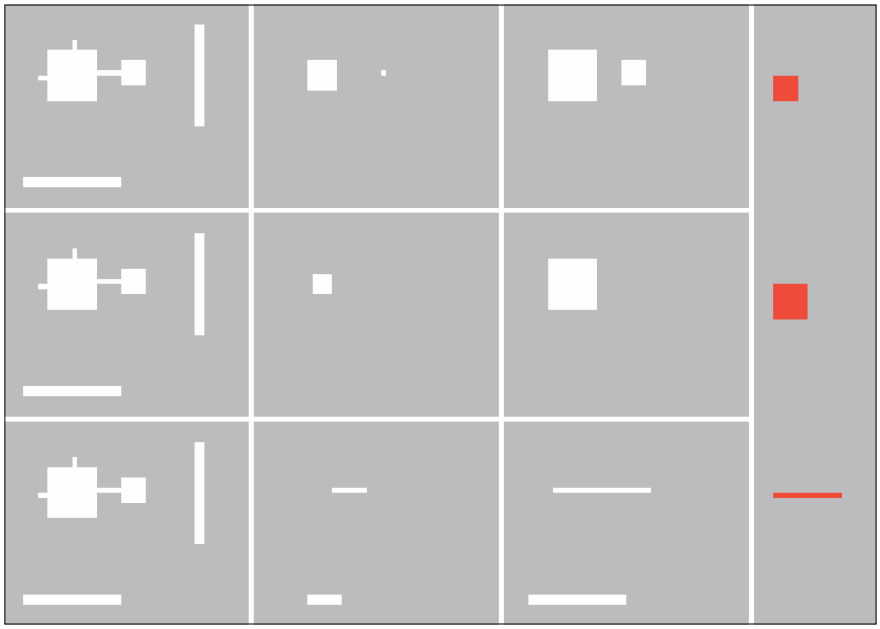

Fig. 12.25. Mathematical morphology example. Pixels are either 0 (grey) or 1 (white). Each column corresponds to processing using the structuring element, shown at the end in red. The first column is the original image, the second column is after erosion by the structuring element, and the third column is after the second column is dilated by the structuring element

resulting pixel will be one. In this case we see that the two squares have returned to their original size, but the large square has lost its protrusions.

Morphological operations are often written in operator form. Erosion is

$$\boldsymbol{O} = \boldsymbol{I} \ominus \mathbb{S}$$

where in Eq. 12.7 $f(\cdot) = \min(\cdot)$, and dilation is

$$\boldsymbol{O} = \boldsymbol{I} \oplus \mathbb{S}$$

where in Eq. 12.7 $f(\cdot) = \max(\cdot)$.

Erosion and dilation are related by

$$A \oplus B = \overline{\bar{A} \ominus B'}$$

where the bar denotes the logical complement of the pixel values and B' indicates the reflection of B about its centre.◀ Essentially this states that eroding the white pixels is the same as dilating the dark pixels and vice versa. The morphological operations are associative

$B'[i,j] = B[j,i]$ where $i = 0, j = 0$ is the centre of the structuring element.

$$(A \oplus B) \oplus C = A \oplus (B \oplus C)$$

$$(A \ominus B) \ominus C = A \ominus (B \oplus C)$$

which means that successive erosion or dilation with a structuring element can be equivalent to the application of a single larger structuring element, but the former is computationally cheaper.◀ These operations are also known as Minkowski subtraction and addition respectively. The shorthand functions

For example a 3×3 square structuring element applied twice is equivalent to 5×5 square structuring element. The former involves $2 \times (3 \times 3 \times N^2) = 18N^2$ operations whereas the later involves $5 \times 5 \times N^2 = 25N^2$ operations.

```
>> out = ierode(im, S);
>> out = idilate(im, S);
```

can be used instead of `imorph`.

Fig. 12.26.
Mathematical morphology example. Pixels are either 0 (grey) or 1 (white). Each row corresponds to processing using the structuring element, shown at the end in red. The first column is the original image, the second column is after dilation by the structuring element, and the third column is after the second column is eroded by the structuring element

The sequence of operations, erosion then dilation, is known as opening since it opens up gaps. In operator form it is written as

$$I \circ S = (I \ominus S) \oplus S$$

Not only has the opening selected particular shapes but it has also *cleaned up* the image: the squares have been separated and the protrusions on the large square have been removed since they are not consistent with the shape of the structuring element.

In Fig. 12.26 we perform the operations in the inverse order, dilation then erosion. In the first row no shapes have been lost, they grew then shrank, and the large square still has its protrusions. The hole has been filled since it is not consistent with the shape of the structuring element. In the second row, the larger structuring element has caused the two squares to join together. This sequence of operations is referred to as closing since it closes gaps and is written in operator form as

$$I \bullet S = (I \oplus S) \ominus S$$

Note that in the bottom row the two line segments have remained attached to the edge, this is due to the default behaviour in handling edge pixels.

Dealing with edge pixels. The problem of a convolution window near the edge of an input image was discussed on page 299. Similar problems exist for morphological spatial operations, and the Toolbox functions `imorph`, `irank` and `iwindow` support the option `'valid'` as does `iconv`. Other options cause the returned image to be the same size as the input image:

- `'replicate'` (default) the border pixel is replicated, that is, the value of the closest border pixel is used.
- `'none'` pixels beyond the border are not included in the set of pixels specified by the structuring element.
- `'wrap'` the image is assumed to wrap around, left to right, top to bottom.

These names make sense when considering what happens to white objects against a black background. For black objects the operations perform the inverse function.

Opening and closing◂ are implemented by the Toolbox functions `iopen` and `iclose` respectively. Unlike erosion and dilation repeated application of opening or closing is futile since those operations are idempotent

$$(I \circ S) \circ S = I \circ S$$
$$(I \bullet S) \bullet S = I \bullet S$$

12.5.1 Noise Removal

A common use of morphological opening is to remove noise in an image. The image

```
>> objects = iread('segmentation.png');
```

Image segmentation and binarization is discussed in Sect. 13.1.1.

shown in Fig. 12.27a is a noisy binary image from the output of a rather poor object segmentation operation.◂ We wish to remove the dark pixels that do not belong to the objects and we wish to fill in the holes in the four dark rectangular objects.

We choose a symmetric *circular* structuring element of radius 3

```
>> S = kcircle(3)
S =
     0     0     0     1     0     0     0
     0     1     1     1     1     1     0
     0     1     1     1     1     1     0
     1     1     1     1     1     1     1
     0     1     1     1     1     1     0
     0     1     1     1     1     1     0
     0     0     0     1     0     0     0
```

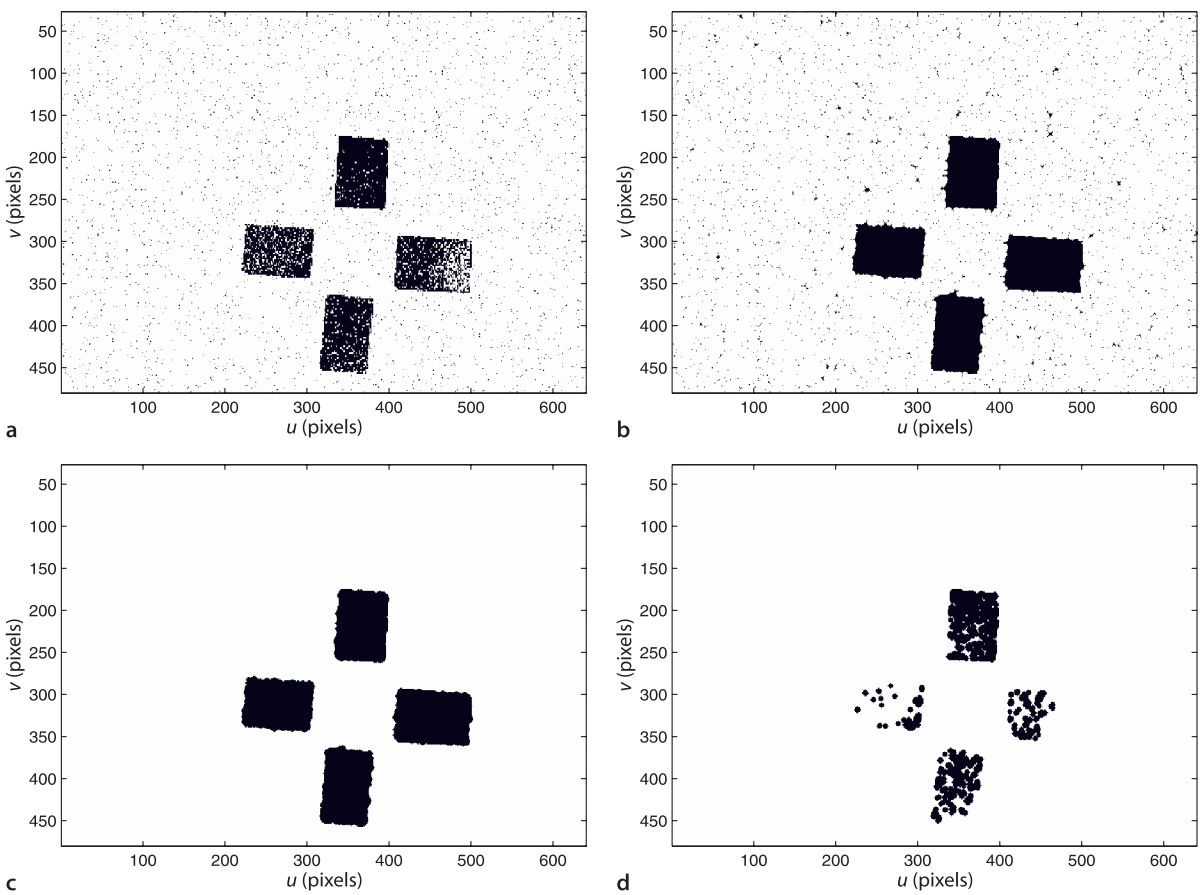

Fig. 12.27. Morphological cleanup. **a** Original image, **b** original after opening, **c** opening then closing, **d** closing then opening. Structuring element is a circle of radius 3

and apply a closing operation to fill the holes in the objects

```
>> closed = iclose(objects, S);
```

and the result is shown in Fig. 12.27b. The holes have been filled, but the noise pixels have grown to be small circles and some have agglomerated. We eliminate these by an opening operation

```
>> clean = iopen(closed, S);
```

and the result shown in Fig. 12.27c is a considerably cleaned up image. If we apply the operations in the inverse order, opening then closing

```
>> opened = iopen(objects, S);
>> closed = iclose(opened, S);
```

the results shown in in Fig. 12.27d are much poorer. Although the opening has removed the isolated noise pixels it has removed large chunks of the targets which cannot be restored.

12.5.2 Boundary Detection

We can also use morphological operations to detect the edges of objects. Continuing the example from above and using the image `clean` shown in Fig. 12.27c we compute its erosion using a circular structuring element

```
>> eroded = imorph(clean, kcircle(1), 'min');
```

The objects in this image are slightly smaller since the structuring element has caused one pixel to be *shaved off* the outside of each object. Subtracting the eroded image from the original

```
>> idisp(clean-eroded)
```

results in a layer of pixels around the edge of each object as shown in Fig. 12.28.

12.5.3 Hit and Miss Transform

The hit and miss transform uses a variation on the morphological structuring element. Its values are zero, one or *don't care* as shown in Fig. 12.29a. The zero and one

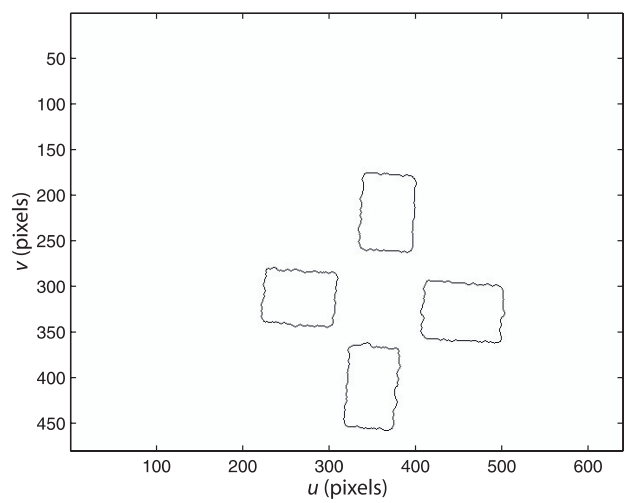

Fig. 12.28.
Boundary detection by morphological processing. Results are shown inverted, white is zero

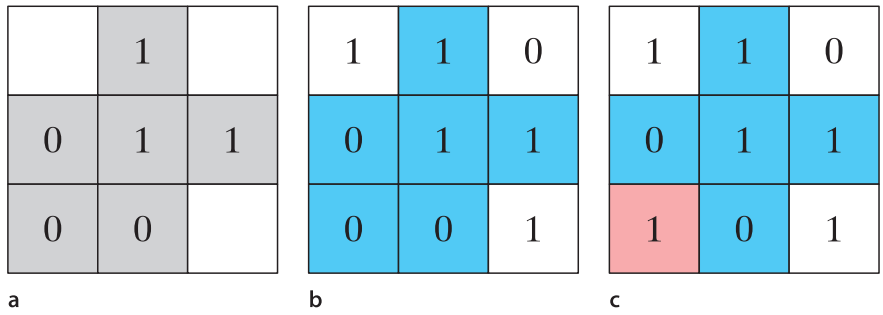

Fig. 12.29. Hit and miss transform. **a** The structuring element has values of zero, one, or don't care which is shown in white; **b** an example of a hit; **c** an example of a miss, the pixel shown in red is inconsistent with the structuring element

pixels must exactly match the underlying image pixels in order for the result to be a one, as shown in Fig. 12.29b. If there is any mismatch of a one or zero as shown in Fig. 12.29c then the result will be zero. The Toolbox implementation is very similar to the morphological function, for example

```
out = hitormiss(image, S);
```

where the don't care elements of the structuring element are set to the special MATLAB® value `NaN`.

The hit and miss transform is used iteratively with a variety of structuring elements to perform operations such as skeletonization and linear feature detection. The skeleton of the objects is computed by

```
>> skeleton = ithin(clean);
```

and is shown in Fig. 12.30a. The lines are a single pixel wide and are the edges of a generalized Voronoi diagram – they delineate sets of pixels according to the shape boundary they are closest to. We can then find the endpoints of the skeleton

```
>> ends = iendpoint(skeleton);
```

and also the triplepoints

```
>> joins = itriplepoint(skeleton);
```

which are points at which three lines join. These are shown in Fig. 12.30b and c respectively.

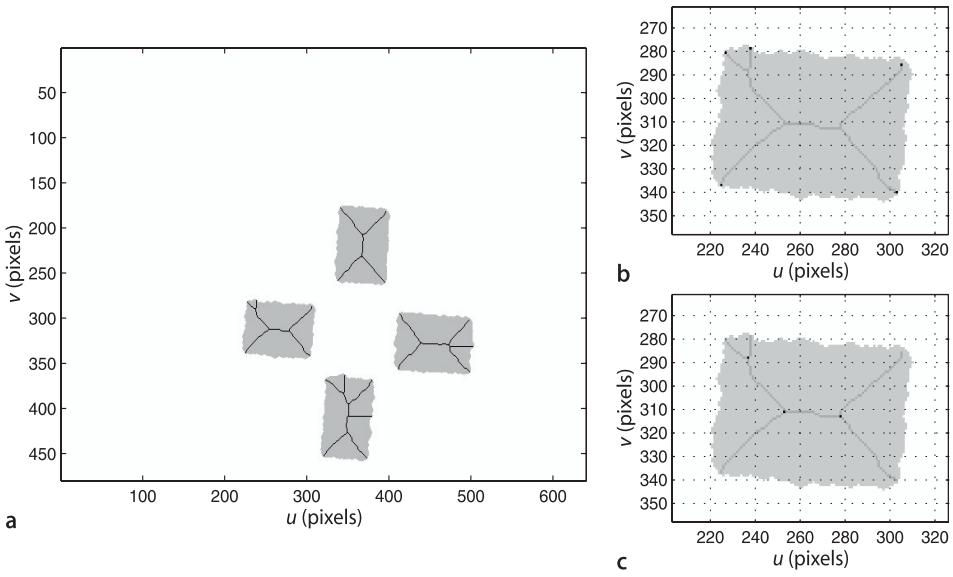

Fig. 12.30. Hit and miss transform operations. **a** Skeletonization; **b** endpoint detection; **c** triple-point join detection. The images are shown inverted with the original binary image superimposed in grey. The end- and triple-points are shown as black pixels

12.6 Shape Changing

The final class of image processing operations that we will discuss are those that change the shape or size of an image.

12.6.1 Cropping

The simplest shape change of all is selecting a rectangular region from an image which is the familiar *cropping* operation. Consider the image

```
>> lena = iread('lena.pgm');
```

shown in Fig. 12.31a from which we interactively specify a region of interest or ROI

```
>> [eyes,roi] = iroi(lena);
>> idisp(eyes)
```

by clicking and dragging a selection box over the image. In this case we selected the eyes as shown in Fig. 12.31b. The corners of the selected region can be optionally returned and in this case was

```
>> roi
roi =
   239   359
   237   294
```

where the columns are the (u, v) coordinates for the top-left and bottom-right corners respectively. The rows are the u- and v-span respectively. The function can be used non-interactively by specifying a ROI

```
>> mouth = iroi(lena, [253, 330; 332, 370]);
```

which in this case selects the mouth.

12.6.2 Image Resizing

Often we wish to reduce the dimensions of an image, perhaps because the large number of pixels results in long processing time or requires too much memory. We demonstrate this with a high-resolution image

```
>> roof = iread('roof.jpg', 'grey');
>> about(roof)
roof [uint8] : 1668x2009 (3351012 bytes)
```

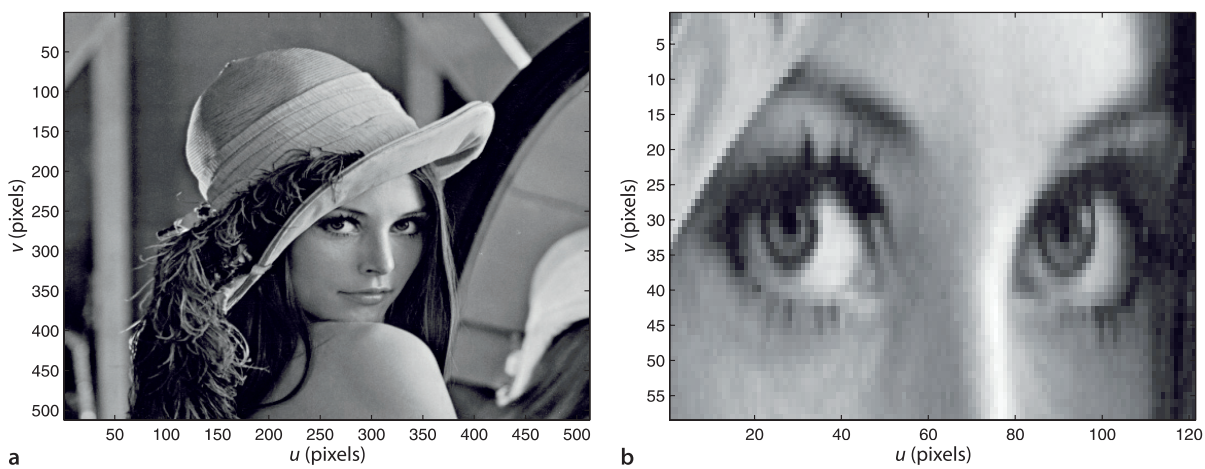

Fig. 12.31. Example of region of interest or image cropping. **a** Original image, **b** selected region of interest

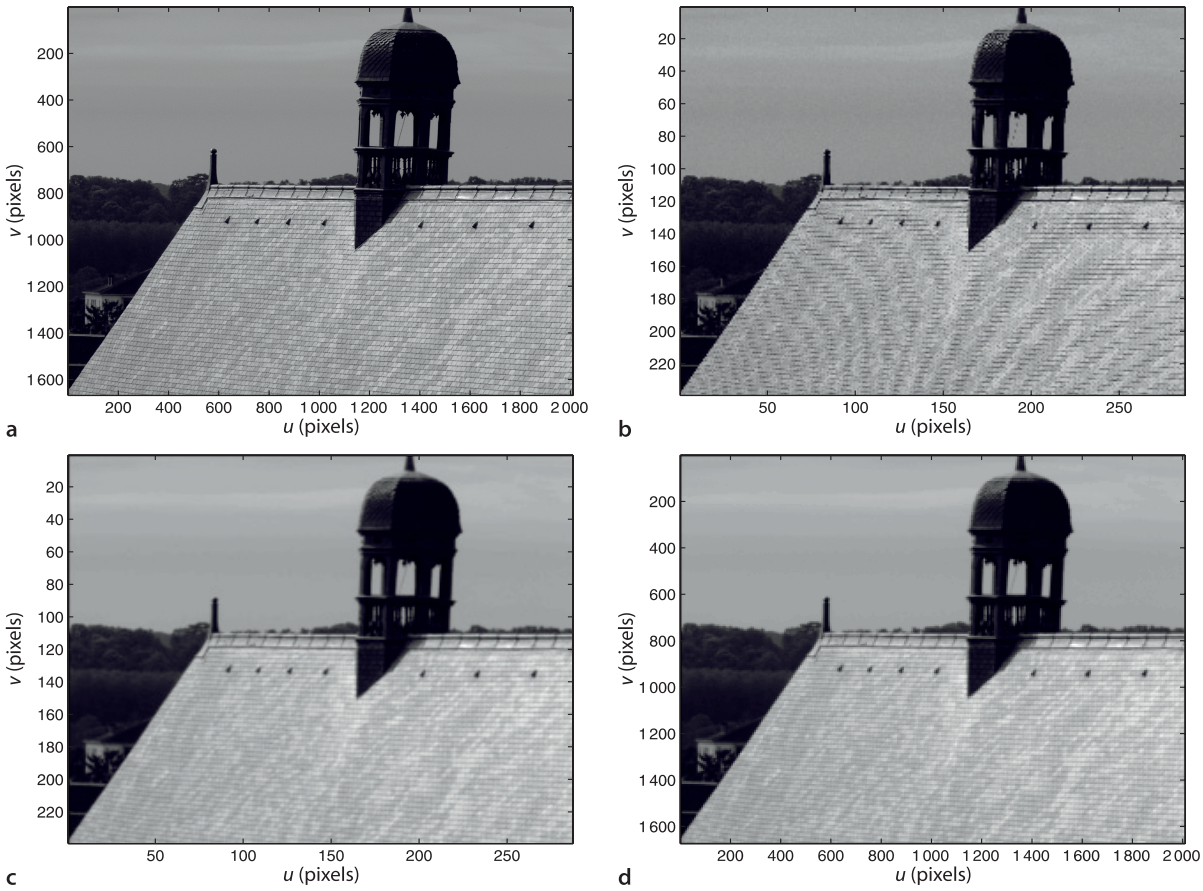

Fig. 12.32. Image scaling example. **a** Original image; **b** subsampled with $m = 7$, note the axis scaling; **c** subsampled with $m = 7$ after smoothing; **d** image **c** restored to original size by pixel replication

which is shown in Fig. 12.32a. The simplest means to reduce image size is subsampling or decimation which selects every m^{th} pixel in the u- and v-direction, where $m \in \mathbb{Z}^+$ is the subsampling factor. For example with $m = 2$ an $N \times N$ image becomes an $N/2 \times N/2$ images which has one quarter the number of pixels of the original image.

For this example we will reduce the image size by a factor of seven in each direction

```
>> smaller = roof(1:7:end,1:7:end);
```

using standard MATLAB® indexing syntax to select every seventh row and column. The result is shown is shown in Fig. 12.32b and we observe some pronounced curved lines on the roof which were not in the original image. These are artefacts of the sampling process. Subsampling reduces the spatial sampling rate of the image which can lead to spatial aliasing of high-frequency components due to texture or sharp edges. To ensure that the Shannon-Nyquist sampling theorem is satisfied an anti-aliasing low-pass spatial filter must be applied to reduce the spatial bandwidth of the image before it is subsampled.◀ This is another use for image blurring and the Gaussian kernel is a suitable low-pass filter for this purpose. The combined operation of smoothing and subsampling is implemented in the Toolbox by

Any realizable low-pass filter has a finite response above its *cutoff* frequency. In practice the cutoff frequency is selected to be far enough below the theoretical cutoff that the filter's response at the Nyquist frequency is *sufficiently* small. As a rule of thumb for subsampling with $m = 2$ a Gaussian with $s = 1$ is used.

```
>> smaller =  idecimate(roof, 7);
```

and the results for $m = 7$ are shown in Fig. 12.32c. We note that the curved line artefacts are no longer present.

The inverse operation is pixel replication, where each input pixel is replicated as an $m \times m$ tile in the output image

```
>> bigger = ireplicate( smaller, 7 );
```

which is shown in Fig. 12.32d and appears a little *blocky* along the edge of the roof and along the skyline. The decimation stage removed 98% of the pixels and restoring the image to its original size has not added any new information. However we could make the image easier on the eye by smoothing

Somewhat like the digital zoom function on a camera.

```
>> smoother = ismooth( bigger, 4);
```

which will attenuate the high frequency information at the edges of the blocks.

We can perform the same function using the Toolbox function `iscale` which scales an image by an arbitrary factor $m \in \mathbb{R}^+$ for example

```
>> smaller = iscale(lena, 0.1);
>> bigger = iscale(smaller, 10);
```

The second argument is the scale factor and if $m < 1$ the image will be reduced, and if $m > 1$ it will be expanded.

The image should be smoothed first using the `'smooth'` option to set the width of the Gaussian kernel.

12.6.3 Image Pyramids

An important concept in computer vision, and one that we return to in the next chapter is scale space. The Toolbox function `ipyramid` returns a pyramidal decomposition of the input image

```
>> p = ipyramid(lena)
p =
  Columns 1 through 5
    [512x512 double]    [256x256 double]    [128x128 double]
    [64x64 double]    [32x32 double]

  Columns 6 through 10
    [16x16 double]    [8x8 double]    [4x4 double]
    [2x2 double]    [20.8959]
```

as a MATLAB® cell array containing images at successively lower resolutions. Note that the last element is the 1×1 resolution version – a single grey pixel! These images are pasted into a composite image which is displayed in Fig. 12.33.

An image pyramid is the basis of many so-called coarse-to-fine strategies. Consider the problem of looking for a pattern of pixel values that represent some object of interest. The smallest image can be searched very quickly for the object since it has a very small number of pixels. The search is then refined using the next larger image but we now know which area of that larger image to search. The process is repeated until the object is located in the highest resolution image.

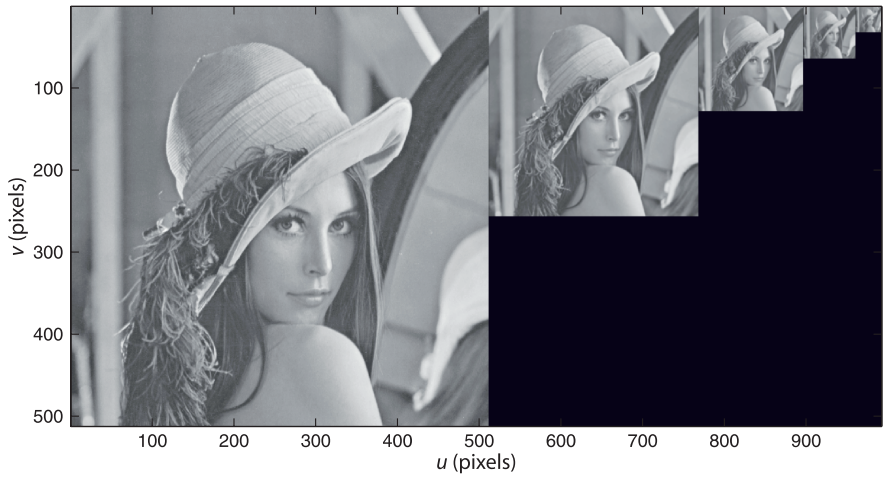

Fig. 12.33. Image pyramid, a succession of images each half (by side length) the resolution of the one to the left

12.6.4 Image Warping

Image warping is a transformation of the pixel *coordinates* not their values. Warping can be used to scale image up or down in size, rotate an image or apply quite arbitrary shape changes. The coordinates of the pixel in the new view (u', v') are expressed as functions

$$u' = f_u(u, v), \quad v' = f_v(u, v) \tag{12.8}$$

of the coordinates in the original view.

Consider a simple example where the image is reduced in size by a factor of 4 in both directions and offset so that its origin, its top-left corner, is shifted to the coordinate (100, 200). We can express this concisely as

$$u' = u/4 + 100, \quad v' = v/4 + 200 \tag{12.9}$$

The coordinate matrices are such that `U(u,v) = u` and `V(u,v) = v` and are a common construct in MATLAB® see the documentation for `meshgrid`.

First we establish a pair of coordinate matrices◀ that span the domain of the input image

```
>> [Ui,Vi] = imeshgrid(lena);
```

and another pair that span the domain of the output image which we choose arbitrarily to be 400×400

```
>> [Uo,Vo] = imeshgrid(400, 400);
```

Now, for *every* pixel in the output image the corresponding coordinate in the input image is given by the inverse of the functions f_u and f_v. For our example the inverse of Eq. 12.9 is

$$u = 4(u' - 100), \quad v = 4(v' - 200) \tag{12.10}$$

which is implemented in matrix form in MATLAB® as

```
>> U = 4*(Uo-100); V = 4*(Vo-200);
```

We can now warp the input image using the MATLAB® function `interp2`

```
>> lena_small = interp2(Ui, Vi, idouble(lena), U, V);
```

and the result is shown in Fig. 12.34a. Note that `interp2` needs to work on a floating point image and we used `idouble` to convert the input image accordingly.

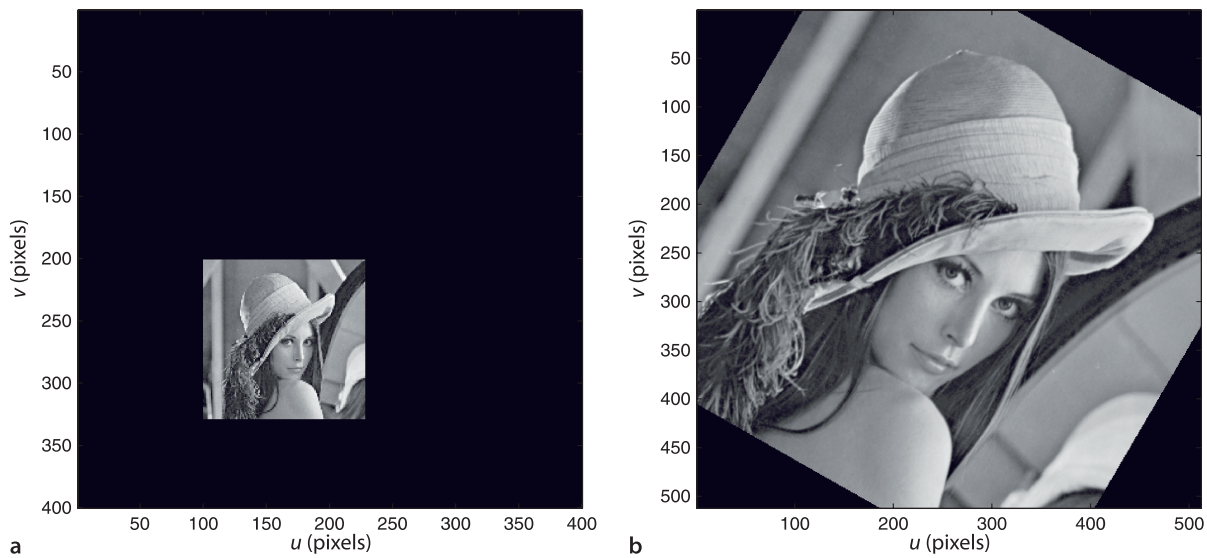

Fig. 12.34. Warped images. **a** Scaled and shifted; **b** rotated by 30° about its centre

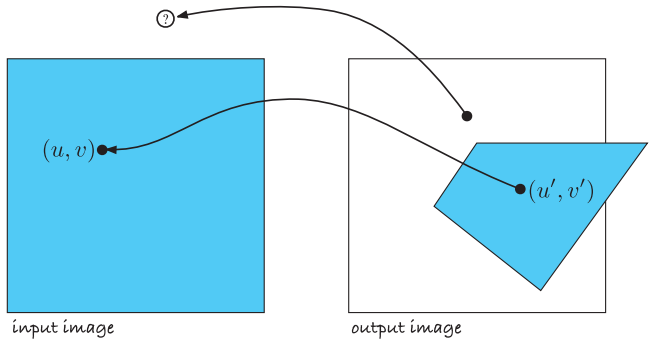

Fig. 12.35.
Coordinate notation for image warping. The pixel (u', v') in the output image is sourced from the pixel at (u, v) in the input image as indicated by the arrow. The warped image is not necessarily polygonal, nor entirely within the second image

Some subtle things happen under the hood here. Firstly, while (u', v') are integer coordinates the input image coordinates (u, v) will not necessarily be integer. The pixel values must be interpolated▶ from neighbouring pixels in the input image◀ Secondly, not all pixels in the output image have corresponding pixels in the input image as illustrated in Fig. 12.35. Fortunately for us `interp2` handles all these issues and pixels that do not exist in the input image are presented as black in the output image. In case of mappings that are extremely distorted it may be that many adjacent output pixels map to the same input pixel and this leads to pixelation or *blockyness* in the output image.

Different interpolation modes can be selected by a trailing argument to `interp2` but the default option is bilinear interpolation. A pixel at coordinate $(u + \delta_u, v + \delta_v)$ where $u, v \in \mathbb{Z}$ and $\delta_u, \delta_v \in [0, 1)$ is a function of the pixels (u, v), $(u + 1, v)$, $(u, v + 1)$ and $(u + 1, v + 1)$.

Now let's try something a bit more ambitious and rotate the image by 30° into an output image of the same size as the input image

```
>> [Uo,Vo] = imeshgrid(lena);
```

We want to rotate the image about its centre but since the origin of the input image is the top-left corner we must first change the origin to the centre, then rotate and then move the origin back to the top-left corner. The warp equation is therefore

$$\begin{pmatrix} u' \\ v' \end{pmatrix} = \underbrace{\begin{pmatrix} \cos\pi/6 & -\sin\pi/6 \\ \sin\pi/6 & \cos\pi/6 \end{pmatrix}}_{R(\pi/6)} \begin{pmatrix} u - u_c \\ v - v_c \end{pmatrix} + \begin{pmatrix} u_c \\ v_c \end{pmatrix} \tag{12.11}$$

where (u_c, v_c) is the coordinate of the image centre and $\boldsymbol{R}(\frac{\pi}{6})$ is a rotation matrix in $SE(2)$. This can be rearranged into the *inverse form* and implemented as

```
>> R = se2(0, 0, pi/6); uc = 256; vc = 256;
>> U = R(1,1)*(Uo-uc) + R(2,1)*(Vo-vc) + uc;
>> V = R(1,2)*(Uo-uc) + R(2,2)*(Vo-vc) + vc;
>> lena_rotated = interp2(Ui, Vi, idouble(lena), U, V);
```

and the result is shown in Fig. 12.34b. Note the direction of rotation – our definition of the x- and y-axes (parallel to the u- and v-axes respectively) is such that the z-axis is defined as being into the page making a clockwise rotation a positive angle. Also note that the corners of the original image have been lost, they fall outside the bounds of the output image.

The function `iscale` uses image warping to change image scale, and the function `irotate` uses warping to perform rotation. The example above could be achieved by

```
>> lena_rotated = irotate(lena, pi/6);
```

The interpolation function acts as a weak anti-aliasing filter, but for very large reductions in scale the image should be smoothed first using a Gaussian kernel.

Finally we will revisit the lens distortion example from Sect. 11.1.1. The distorted image from the camera is the input image and will be warped to remove the distortion. We are in luck since the distortion model Eq. 11.13 is already in the inverse form. Recall that

$$u^d = u + \delta_u$$
$$v^d = v + \delta_v$$

where δ_u and δ_v are functions of (u, v).

First we load the distorted image and build the coordinate matrices for the distorted and undistorted images

```
>> distorted = iread('Image18.tif', 'double');
>> [Ui,Vi] = imeshgrid(distorted);
>> Uo = Ui; Vo = Vi;
```

and then load the results of the camera calibration

```
>> load  Bouguet
```

For readability we unpack the required parameters from the Calibration Toolbox variables `cc`, `fc` and `kc`

```
>> k = kc([1 2 5]); p = kc([3 4]);
>> u0 = cc(1); v0 = cc(2); fpix_u = fc(1); fpix_v = fc(2);
```

for radial and tangential distortion vectors, principal point and focal length in pixels. Next we convert pixel coordinates to normalized image coordinates◂

In units of metres with respect to the camera's principal point.

```
>> u = (Uo-u0) / fpix_u;
>> v = (Vo-v0) / fpix_v;
```

The radial distance of the pixels from the principal point is then

```
>> r = sqrt( u.^2 + v.^2 );
```

and the pixel coordinate errors due to distortion are

```
>> delta_u = u .* (k(1)*r.^2 + k(2)*r.^4 + k(3)*r.^6) + ...
   2*p(1)*u.*v + p(2)*(r.^2 + 2*u.^2);
>> delta_v = v .* (k(1)*r.^2 + k(2)*r.^4 + k(3)*r.^6) + ...
   p(1)*(r.^2 + 2*v.^2) + 2*p(1)*u.*v;
```

The distorted pixel coordinates in metric units are

```
>> ud = u + delta_u;  vd = v + delta_v;
```

which we convert back to pixel coordinates

```
>> U = ud * fpix_u + u0;
>> V = vd * fpix_v + v0;
```

and finally apply the warp

```
>> undistorted = interp2(Ui, Vi, distorted, U, V);
```

The results are shown in Fig. 12.36. The change is quite subtle, but is most pronounced at the edges and corners of the image where r is the greatest.

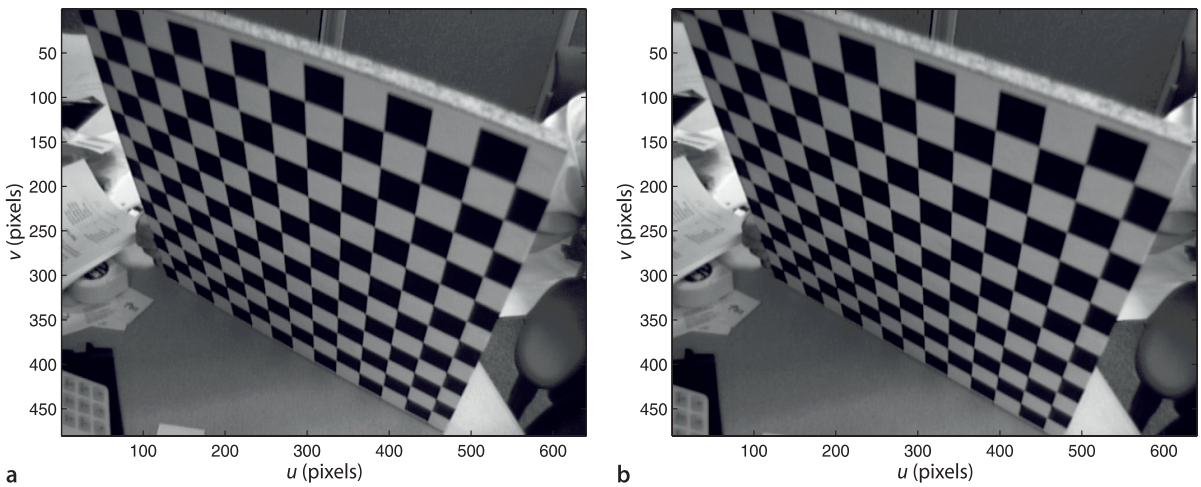

Fig. 12.36. Warping to undistort an image. **a** Original distorted image; **b** corrected image. Note that the top edge of the target has become a straight lines (Example from Bouguet's Camera Calibration Toolbox, image number 18)

12.7 Wrapping Up

In this chapter we learnt how to acquire images from a variety of sources such as image files, movie files, video cameras and the internet, and load them into the MATLAB® workspace. We then discussed a large number of processing operations and a taxonomy of these is shown in Fig. 12.37. Operations on a single image include: unary arithmetic operations, type conversion, various color transformations and greylevel stretching; non-linear operations such as histogram normalization and gamma encoding or decoding; and logical operations such as thresholding. We also discussed operations on pairs of images such as green screening, background estimation and moving object detection.

The largest and most diverse class of operations were spatial operators. We discussed convolution which can be used to smooth an image and to detect edges. Smoothing is useful to reduce the effect of image noise in edge detection and also to low-pass filter an image prior to decimation. Non-linear operations can be used to perform template matching and to compute rank statistics over windows. A particular example of rank statistics is the median filter which was shown to reduce certain types of image noise. A related technique is mathematical morphology which can be used to filter images based on shape, to cleanup binary images and to perform skeletonization.

Finally we discussed shape changing operations such as regions of interest, scale changing and the problems that can arise due to aliasing, and generalized image warping which can be used for rotation or image undistortion. All these image processing techniques are the foundations of feature extraction algorithms that we discuss in the next chapter.

Further Reading

Image processing is a large field and this chapter has provided an introduction to many of the most useful techniques from a robotics perspective. The textbook by Gonzalez and Woods (2008) has a comprehensive discussion of image processing techniques as does Szeliski (2011). It expands on methods introduced in this chapter and covers additional topics such as greyscale morphology, image restoration, wavelet and frequency domain methods, and image compression. Online information about computer vision is available through CVonline at http://homepages.inf.ed.ac.uk/rbf/CVonline, and the material in this chapter is covered under the section *Image Transformations and Filters*.

Edge detection is a subset of image processing but one with huge literature of its own. Forsyth and Ponce (2002) have a comprehensive introduction to edge detection and a useful discussion on the limitations of edge detection. Nixon and Aguado (2008) also cover phase congruency approaches to edge detection and compare various edge detectors. The Sobel kernel for edge detection was described in an unpublished 1968 publication from the Stanford AI lab by Irwin Sobel and Jerome Feldman: *A 3 × 3 Isotropic Gradient Operator for Image Processing*. The Canny edge detector was originally described in Canny (1983, 1987).

Non-parametric measures for image similarity became popular in the 1990s with with a number of key papers such as Zabih and Woodfill (1994), Banks and Corke (2001), Bhat and Nayar (2002). The application to real-time image processing systems using high-speed logic such as FPGAs has been explored by several groups (Corke et al. 1999; Woodfill and Von Herzen 1997).

Mathematical morphology is another very large topic and we have only scraped the surface. Important techniques such as greyscale morphology and watersheds have not been covered. The pioneer of the field is Jean Serra and good starting points for further investigation are his book from 1983 (Serra 1983) or online tutorials at the Centre for Mathematical Morphology at http://cmm.ensmp.fr/index_eng.html. Another thorough treatment is the book by Soille (2003) while the book by Dougherty and Latufo (2003) is a more hands on tutorial approach. Gonzalez and Woods also has a useful discussion of greyscale morphology.

Fig. 12.37. Taxonomy of image processing algorithms discussed in this chapter

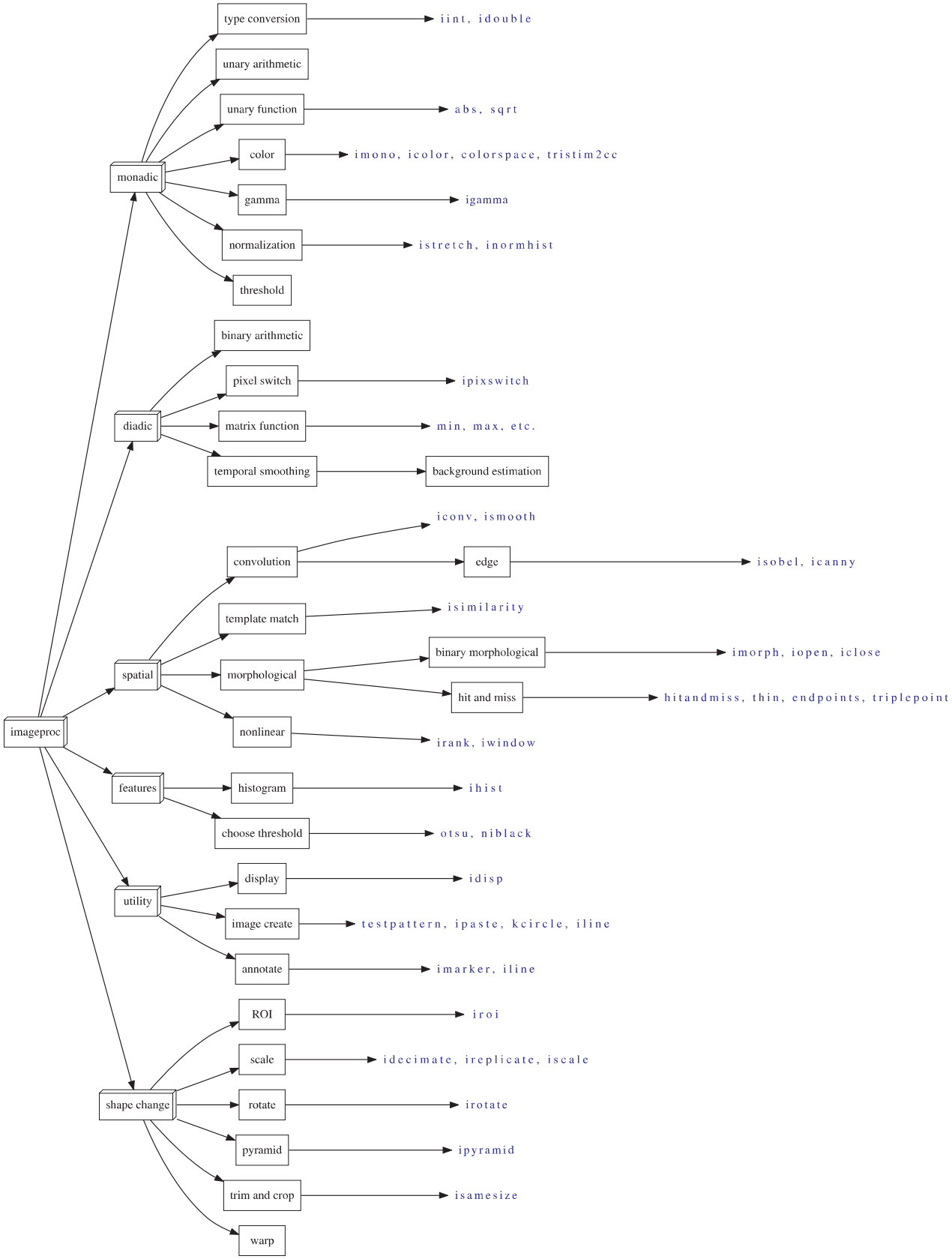
imageproc
monadic
type conversion
iint, idouble
unary arithmetic
unary function
abs, sqrt
color
imono, icolor, colorspace, tristim2cc
gamma
igamma
normalization
istretch, inormhist
threshold
diadic
binary arithmetic
pixel switch
ipixswitch
matrix function
min, max, etc.
temporal smoothing
background estimation
spatial
convolution
iconv, ismooth
edge
isobel, icanny
template match
isimilarity
morphological
binary morphological
imorph, iopen, iclose
hit and miss
hitandmiss, thin, endpoints, triplepoint
nonlinear
irank, iwindow
features
histogram
ihist
choose threshold
otsu, niblack
utility
display
idisp
image create
testpattern, ipaste, kcircle, iline
annotate
imarker, iline
shape change
ROI
iroi
scale
idecimate, ireplicate, iscale
rotate
irotate
pyramid
ipyramid
trim and crop
isamesize
warp

The approach to compute vision covered in this book is often referred to as bottom-up processing. This chapter has been about *low-level* vision techniques which are operations on pixels. The next chapter is about *high-level* vision techniques where sets of pixels are grouped and then described to represent objects in the scene.

Sources of Image Data

There are thousands of online webcams as well as a number of sites that aggregate web cameras and provide lists categorized by location. Some of the content on these list pages can be rather dubious – so beware. Most of these sites do not connect you directly to the web camera so the URL of the camera is generally not available. Sites such as Opentopia http://www.opentopia.com do list a large number of web cameras and the actual URL for the camera is listed below the image on the line marked *Website:*. The the root part of the URL (before the first single slash) is required for the `AxisWebCamera` class.

The motion sequence videos used in Sect. 12.3 are available from the CAVIAR project at http://homepages.inf.ed.ac.uk/rbf/CAVIARDATA1 and are described in Fisher (2004).

A number of images are provided with the Toolbox in the `images` folder.

MATLAB® Software Tools

The Image Processing Toolbox (IPT) can be purchased from The Mathwork Inc., the publishers of MATLAB. The companion to Gonzalez and Woods (2008) is their MATLAB® based book from 2009 (Gonzalez et al. 2009) which provides a detailed coverage of image processing using MATLAB® and includes functions that extend the IPT. These are provided for free as P-code format (no source or help available) or as M-files for purchase.

The Machine Vision Toolbox (MVTB) described in this book is open source. The MVTB functionality overlaps the IPT, but the MVTB contains functions not in the IPT and the IPT contains functions not in the MVTB. The image processing category at MATLAB® CENTRAL http://www.mathworks.com/matlabcentral/fileexchange lists more than 500 files.

General Software Tools

There is a wealth of high quality software tools for image and video manipulation outside the MATLAB® environment. OpenCV at http://opencv.org is a mature open-source computer vision software project. The book by Bradski and Kaehler (2008) is a good introduction to the software and to computer vision in general.

ImageMagick http://www.imagemagick.org is a cross-platform collection of libraries and command-line tools for image format conversion (over 100 formats), manipulation and composition and the API has bindings for many languages. NetPBM http://netpbm.sourceforge.net can be built on most platforms and is also a collection of command-line tools for image format conversion (over 100 formats) and manipulation. The NetPBM utilities are an install option for many Linux distributions. Both packages are well suited for batch operations on large sets of images. The Toolbox function `pnmfilt` can be used to process an image through one of these external programs, for example

```
>> rlena = pnmfilt(lena, 'pnmrotate 30');
```

For video manipulation FFmpeg http://www.ffmpeg.org is an excellent and comprehensive cross-platform tool. It supports conversion between video formats as well as videos to still images and vice versa.

Exercises

1. Become familiar with `idisp` for greyscale and color images. Explore pixel values in the image as well as the zoom, line and histogram buttons.
2. Grab some frames from the camera on your computer or from a movie file and display them.
3. Write a loop that grabs a frame from your camera and displays it. Add some effects to the image before display such as "negative image", thresholding, posterization, false color, edge filtering etc.
4. Motion detection
   a) Write a loop that performs background estimation using frames from your camera. What happens as you move objects in the scene, or let them sit there for a while? Explore the effect of changing the parameter σ.
   b) Modify the *LeftBag* example on page 298 and highlight the moving people.
   c) Combine motion detection and chroma-keying, put the moving people from the lobby into the desert.
5. Convolution
   a) Compare the results of smoothing using a 21×21 uniform kernel and a Gaussian kernel. Can you observe the ringing artefact in the former?
   b) Why do we choose a smoothing kernel that sums to one?
   c) Compare the performance of the simple horizontal gradient kernel $\boldsymbol{K} = (-0.5\ 0\ 0.5)$ with the Sobel kernel.
   d) Investigate filtering with the Gaussian kernel for different values of σ and kernel size.
   e) Create a 31×31 kernel to detect lines at 60 deg.
   f) Derive analytically the derivative of the Gaussian in the x-direction Eq. 12.2.
   g) Derive analytically the derivative of the Laplacian of Gaussian Eq. 12.6.
   h) Derive analytically the difference of Gaussian from page 310.
6. Show analytically the effect of an intensity scale error on the SSD and NCC similarity measures.
7. Template matching
   a) Use `iroi` to select one of Lena's eyes as a template. The template should have odd dimensions.
   b) Use `isimilarity` to compute the similarity image. What is the best match and where does it occur? What is the similarity to the other eye? Where does the second best match occur and what is its similarity score?
   c) Scale the intensity of the Lena image and investigate the effect on the peak similarity.
   d) Add an offset to the intensity of the Lena image and investigate the effect on the peak similarity.
   e) Repeat steps *(c)* and *(d)* for different similarity measures such as SAD, SSD, rank and census.
   f) Scale the template size by different factors (use `iscale`) in the range 0.5 to 2.0 in steps of 0.05 and investigate the effect on the peak similarity. Plot peak similarity vs scale.
   g) Repeat *(f)* for rotation of the template in the range -0.2 to 0.2 rad in steps of 0.05.
8. Perform the sub-sampling example on page 325 and examine aliasing artefacts around sharp edges and the regular texture of the roof tiles. What is the appropriate smoothing kernel width for a decimation by M?
9. Write a function to create Fig. 12.33 from the output of `ipyramid`.
10. Create a warp function that mimics your favourite funhouse mirror.
11. Warp the image to polar coordinates (r, θ) with respect to the centre of the image, where the horizontal axis is r and the vertical axis is θ.